The Nature of Star Formation at 24μm in the Group Environment at $0.3 \lesssim z \lesssim 0.55$

K. D. Tyler[1], G. H. Rieke[1], D. J. Wilman[2], S. L. McGee[3,4], R. G. Bower[4], L. Bai,[5], J. S. Mulchaey[5], L. C. Parker[6], Y. Shi[1] D. Pierini[2]

ABSTRACT

Galaxy star formation rates (SFRs) are sensitive to the local environment; for example, the high-density regions at the cores of dense clusters are known to suppress star formation. It has been suggested that galaxy transformation occurs largely in groups, which are the intermediate step in density between field and cluster environments. In this paper, we use deep MIPS 24μm observations of intermediate-redshift ($0.3 \lesssim z \lesssim 0.55$) group and field galaxies from the Group Environment and Evolution Collaboration (GEEC) subset of the Second Canadian Network for Observational Cosmology (CNOC2) survey to probe the moderate-density environment of groups, wherein the majority of galaxies are found. The completeness limit of our study is $\log(L_{TIR}(L_\odot)) \gtrsim 10.5$, corresponding to SFR $\gtrsim 2.7\, M_\odot\, yr^{-1}$. We find that the group and field galaxies have different distributions of morphologies and mass. However, individual group galaxies have star-forming properties comparable to those of field galaxies of similar mass and morphology; that is, the group environment does not appear to modify the properties of these galaxies directly. There is a relatively large number of massive early-type group spirals, along with E/S0 galaxies, that are forming stars above our detection limit. These galaxies account for the nearly comparable level of star-forming activity in groups as compared with the field, despite the differences in mass and morphology distributions between the two environments. The

[1]Steward Observatory, University of Arizona, 933 N. Cherry Ave., Tucson, AZ 85721, USA

[2]Max-Planck-Institut für extraterrestrische Physik, Giessenbachstraße, D-85748 Garching, Germany

[3]Department of Physics and Astronomy, University of Waterloo, Waterloo, Ontario, N2L 3G1, Canada

[4]Institute for Computational Cosmology, Department of Physics, Durham University, South Road, Durham DH1 3LE, UK

[5]Observatories of the Carnegie Institution, 813 Santa Barbara Street, Pasadena, CA, USA

[6]Department of Physics and Astronomy, McMaster University, 1280 Main Street West, Hamilton, Ontario, L8S 4M1, Canada

distribution of specific SFRs (SFR/M_*) is shifted to lower values in the groups, reflecting the fact that groups contain a higher proportion of massive and less active galaxies. Considering the distributions of morphology, mass, and SFR, the group members appear to lie between field and cluster galaxies in overall properties.

Subject headings: galaxies: evolution - galaxies: photometry - infrared: galaxies

1. INTRODUCTION

In a ΛCDM universe, galaxies, on average, move from areas of lower density to areas of higher density, merging and combining to form larger and larger systems like the massive galaxy clusters we see in the local universe. Galaxy evolution, therefore, cannot be understood without considering the influence of environment on galaxy properties. The importance of environment on galaxy evolution is demonstrated by the differences between galaxies in clusters and those in the field. For example, the fraction of blue galaxies in clusters has been decreasing since $z \sim 1$, and local clusters are dominated by red galaxies (Butcher & Oemler 1978; Kennicutt 1983; Hashimoto et al. 1998; Andreon et al. 2004; Poggianti et al. 2006; Cooper et al. 2007; Loh et al. 2008; Cucciati et al. 2010). Dressler (1980) found a dramatic increase in the proportion of early-type galaxies with local density inside rich clusters, i.e., the morphology-density relation. This relation has also been shown to extend down to the group environment (Postman & Geller 1984). Most of these cluster early-type galaxies have not had appreciable star formation in gigayears, though as we move outward from the centers of the clusters, we see more late-type galaxies overall and more early-type galaxies that have had more recent star formation (Balogh et al. 1997, 1999; Bai et al. 2009).

Environment is expected to influence the rates of both gas exhaustion and interactions. The drop in star-forming activity in dense environments might be due to interactions with the inter-galactic gas, such as through ram-pressure stripping of cold gas in galaxies (Gunn & Gott 1972; Larson et al. 1980; Kinney et al. 2004) or stripping of the hot gas through strangulation (Balogh et al. 2000; Kawata & Mulchaey 2008; McCarthy et al. 2008). Alternatively, the lower fraction of star forming galaxies might arise through galaxy-galaxy interactions, either major mergers or harassment (frequent high-speed encounters of galaxies that do not lead to mergers), both of which would accelerate the star formation and lead to early exhaustion of the interstellar material. Tides raised by the overall gravitational potential of dense clusters may also play a role (Henriksen & Byrd 1996). It has been proposed that the morphological transformation into early-type galaxies may occur first,

suppressing star formation by stabilizing the gas against fragmentation (Martig et al. 2009), although other recent studies question this claim (Kovač et al. 2010).

Explaining the behavior of galaxies in different environments in terms of consistent theories for the growth of galaxies in the early universe has proven challenging (Bower et al. 2006; Kaviraj et al. 2009). Therefore, an intense observational approach is needed to help develop an understanding of the relation between environment and galaxy evolution. It should be possible to disentangle environmental influences by comparing galaxy behavior in different environments, though just as the mechanisms for galaxy transformation are not fully understood, the environments where these processes operate also need to be explored and defined. Additionally, most of the previous work regarding star formation with respect to environment focused on rich clusters (e.g., Dressler et al. 2009; Bai et al. 2009; Haines et al. 2009, and references therein); relatively few studies have focused on groups (e.g. Zabludoff & Mulchaey 1998, 2000; Balogh et al. 2004; Johnson et al. 2007; Marcillac et al. 2008; Bai et al. 2010).

Simard et al. (2009) argue that cluster-centric processes are not the dominant factor in galaxy morphological transformation. The majority of galaxies live in the less-dense group environment (Geller & Huchra 1983; Eke et al 2004), and because clusters probably form from coalescing groups and field galaxies, much of the evolution apparent in cluster galaxies may have occurred in groups prior to their assimilation into clusters. Zabludoff & Mulchaey (1998) found that the proportion of early-type galaxies in groups ranged from that typical of the field ($\sim$25%) to that found in dense clusters ($\sim$55%), suggesting that much of the morphological transformation of galaxies from field to cluster properties occurs in groups. Just et al. (2010) show that an increase in the proportion of S0 galaxies with decreasing redshift occurs in moderate-mass groups/poor clusters ($\sigma < 750$ km s^{-1}), and Wilman et al. (2009) find that for groups at intermediate redshifts, the fraction of S0s is as high as in clusters, even at fixed luminosities. Additionally, because most galaxies reside in groups—and, therefore, galaxies spend most of their time in groups—uncovering the effects of these lower-density environments can help us understand the evolutionary path of the global galaxy population over cosmic time (McGee et al. 2009).

If morphological transformations frequently occur at intermediate densities, is this also the location where star formation is cutoff? Previous studies of star formation in groups have mostly focused on optical indicators such as Hα or [OII]λ3727 emission lines or ultraviolet continuum. These measures can extend to low levels of star formation, and they indicate a significantly lower level of activity in groups and clusters than in the field (Wilman et al. 2005a; Gerke et al. 2007; Balogh et al. 2009; Iovino et al. 2010; Peng et al. 2010). Such first-order comparisons are usually made under the assumption that the extinction is

similar in groups and clusters (and that star formation is not deeply obscured). However, corrections are required to convert these optical indicators to accurate star formation rates (SFRs). At z $\gtrsim$ 0.3, Hα moves out of the range of optical spectroscopy and SFR estimates rely on [OII], where the extinction is large and uncertain. The [OII]λ3727 line has additional problems of being sensitive to dust reddening and metallicity, thus being relatively weak in high-mass systems, although empirical corrections have been suggested to correct for this and other effects (Moustakas et al. 2006; Gilbank et al. 2010).

The infrared (IR) is advantageous for probing high levels of star formation. While SFRs determined in the IR are only sensitive to dust-obscured star formation, the correction to the total star formation in objects at moderate to high luminosities ($L_{TIR} \gtrsim 1 \times 10^{10}$ $L_\odot$) is small (Rieke et al. 2009). Nonetheless, previous IR studies have not reached consistent conclusions about star formation in groups. Marcillac et al. (2008) found no significant dependence on the incidence of luminous infrared galaxies (LIRGs) as a function of field or group environment at z $\sim$ 0.8. At lower redshifts, Wilman et al. (2008) find a dearth of star formation in group galaxies at z $\sim$ 0.4, while Tran et al. (2009) find a similar incidence of SFRs in massive groups (for galaxies forming stars $> 3M_\odot$ yr^{-1}) as in the field at z $\sim$ 0.37. For local groups, Bai et al. (2010) report rates of star formation somewhat lower than in the field (by $\sim$30%).

This paper is a step toward understanding the influence of the group environment on star formation and resolving some of the apparent discrepancies in previous studies of the same topic. Some of these discrepancies, especially in cluster studies, may arise from "field" samples contaminated by groups. To compare groups with actual field galaxies, we need a clean field sample with as many galaxies as possible. Here, we present 24μm measurements of 232 group galaxies and 236 field galaxies from 0.3 $\lesssim$ z $\lesssim$ 0.55 in the Second Canadian Network for Observational Cosmology (CNOC2) survey.

The paper is organized as follows. In Section 2, we discuss the sample, data reductions, and errors. Section 3 covers the construction of fractional IR luminosity functions (LFs) and compares the IR luminosities, morphologies, and masses of group and field galaxies to estimate what effect (if any) environment has on star formation at these redshifts. We discuss the implications of our results in Section 4. For all cosmological corrections, we assume the parameters H_0 =70 km s^{-1}Mpc^{-1}, $\Omega_M = 0.3,\ \Omega_\Lambda = 0.7$.

2. SAMPLE AND DATA REDUCTION

2.1. Sample Selection and Photometry

The CNOC2 survey is a photometric and spectroscopic survey of faint galaxies covering more than 1.5 deg^2 over four widely-spaced patches of sky (Yee et al. 2000; Carlberg et al. 2001a). The original survey included five-color photometry in I_C, R_C, V, B, and U to $R_C \sim$ 23.0 (Vega) mag and spectroscopic redshifts (to $R_C \sim 21.5$ mag) for an unbiased sample of ∼6000 galaxies with the purpose of studying galaxy clustering, dynamics and evolution at intermediate redshifts ($0.1 \lesssim z \lesssim 0.6$). The survey is spectroscopically incomplete, but the selection function is very well defined for this redshift range (Lin et al. 1999; Yee et al. 2000).

The groups themselves were originally selected by using a friends-of-friends algorithm to find overdensities of galaxies in three-dimensional space (Carlberg et al. 2001a, 2001b). Follow-up LDSS2 spectroscopy (to $R_C \sim 22.0$) targeted 26 of these Carlberg groups at $0.3 \lesssim z \lesssim 0.55$, creating a sample of group and field galaxies to a greater depth than the original sample, with increased and unbiased spectroscopic completeness (Wilman et al. 2005b). Additional group members were carefully selected to ensure that the resulting sample would be unbiased with regard to color using the method outlined in Wilman et al. (2005a). This subset of the original CNOC2 survey—26 groups at $0.3 \lesssim$ z $\lesssim 0.55$ to $R_C \sim$ 22.0—was followed up by the Group Environment and Evolution Collaboration (GEEC), and hereafter, we refer to these as the GEEC groups. Visual (Wilman et al. 2009) and automated (McGee et al. 2008) morphological classifications were made using deep, high-resolution *Hubble Space Telescope* (HST) Advanced Camera for Surveys (ACS) images of the same 26 groups (Wilman et al. 2009). Additional multiwavelength coverage includes *Galaxy Evolution Explorer* (GALEX) UV (McGee et al. 2011), and IRAC (Balogh et al. 2007, 2009; Wilman et al. 2008). X-ray properties of a subset of the groups have been measured with *XMM-Newton* and *Chandra* observations (Finoguenov et al. 2009).

We present observations of these GEEC groups (as defined by Wilman et al. (2005a)) using the MIPS 24μm band on the *Spitzer Space Telescope* (Rieke et al. 2004). We used MIPS in single-source photometry mode (field of $5' \times 5'$) due to the compact nature of the groups, and long exposure times allowed us to detect relatively low SFRs (< 10 M$_\odot$ yr^{-1}). All but five of the groups have either complete coverage of their members with MIPS or are only missing one or two member galaxies. All galaxies assigned to groups using the algorithm described by Wilman et al. (2005a) and within the MIPS field of view are considered group members in this paper. The MIPS 24μm field of view corresponds to ∼1.3 Mpc (∼2 Mpc) on a side at z = 0.3 (0.55).

The data from these observations were reduced using version 3.10 of the MIPS Data Analysis Tool (DAT; Gordon et al. 2007). Fields with overlapping regions were mosaicked for better coverage near the image edges. Sources 3σ above the standard deviation of the background were identified using DAOFIND in the IRAF[2] environment. Flux densities were calculated using a point-spread function (PSF) made from bright sources in one of the larger mosaicked fields and the IRAF PSF-fitting routine ALLSTAR, correcting for flux lost in the wings of the PSF as described by the Spitzer Science Center[3].

Our initial field sample consisted of all galaxies not identified as residing in a group. Given the completeness of the group sample, it has been estimated that ∼21% of this field sample is contaminated by unidentified groups (Carlberg et al. 2001a, McGee et al. 2008). To reduce the amount of group contamination in the field, we plotted a running-average histogram of redshifts for the LDSS2 pencil-beam fields with a bin size of z = 0.001. Any galaxies that fall in a bin with five or more galaxies at any point in the running average were removed from the field sample as possible group contaminants. This method will obviously remove some true field galaxies, as it does not account for the spatial positions of the possible group galaxies; however, this is a quick, simple method for removing galaxies that are likely to live in groups. We removed a total of 78 galaxies—or ∼25%—of our original field sample.

These observations of groups and the "cleaned" field sample (referred to simply as the "field" from this point on) result in 24μm measurements or upper limits for 232 group galaxies and 236 field galaxies from $0.3 \lesssim z \lesssim 0.55$, of which 79 group galaxies and 65 field galaxies are detected. Our absolute detection limit (3σ) is 119μJy, corresponding to the 24μm observations with the highest background. These observations result in a detection limit for the groups of of $L_{TIR} \sim 3.5 \times 10^{10}$ $L_\odot$ (SFR ~ 3.3 $M_\odot$ yr^{-1}), where L_{TIR} is the total IR luminosity as defined by Rieke et al. (2009). However, only two groups (20 galaxies) have detection limits at this level; ∼91% of our group sample (and ∼93% of the field sample) have 24μm coverage to a lower detection limit: $L_{TIR} \sim 2.9 \times 10^{10}$ $L_\odot$ (SFR ~ 2.7 $M_\odot$ yr^{-1}). We use this lower value as our detection limit for the rest of the paper. At a typical redshift for our groups (z ∼ 0.43), L^*_{TIR} corresponds to SFR ~ 10 $M_\odot$ yr^{-1} (Rujopakarn et al. 2010). The typical optical surface density of the GEEC groups is ∼3 galaxies Mpc^{-2} for galaxies with $M_{B_J} <$ -20, though it ranges from ∼1 to ∼6.5. Cluster surface densities can range from these values in the outskirts to as high as several hundred galaxies Mpc^{-2} in the dense cores (Dressler 1980).

[2]IRAF is distributed and supported by the National Optical Astronomy Observatories (NOAO).

[3]The Spitzer Science Center (http://ssc.spitzer.caltech.edu) is supported by NASA, the Jet Propulsion Laboratory, the California Institute of Technology, and the Infrared Processing and Analysis Center.

2.2. Uncertainties and Reliability

We cross-correlated the sources detected at 24μm (almost 2000 objects over all fields) with the GEEC spectroscopic catalog to within 3 arcsec; if multiple optical sources were located within 3 arcsec of a 24μm source, the nearest optical source was used (only 20 instances of such multiple matches using the entire 24μm and CNOC2 catalogs were recorded). Any GEEC galaxy not matching this criterion was given a 3σ upper limit. To estimate the 1σ errors (and 3σ upper limits for non-detected sources) in the 24μm flux densities, we put down apertures in blank areas of the fields and took the standard deviation of the nearest 20 background apertures to a given source.

Because of the depth of our observations and the size of the MIPS 24μm PSF, it is necessary to know the fraction of false detections—in other words, the fraction of 24μm sources incorrectly attributed to an optical source in our catalog. We therefore placed a random number of fake sources (up to 300 sources per pointing, which at z = 0.55 equates a surface density of 4 Mpc^{-2}) on each image and matched the 24μm detections to both the fake source catalog and our GEEC spectroscopic catalog. We use three different match radii—4, 3, and 2.5 arcsec—and found the mean fraction of false detections to be 3.1%, 1.8%, and 1.3%, respectively, for each match radius. As expected, the number of false detections per unit area is relatively constant and does not change significantly for each match radius. We could use any of the listed match radii and not change the number of false matches substantially (i.e. from $\sim$3 to $\sim$7 for the group and field samples individually, out of $\sim$230 galaxies in each environment, and from $\sim$2 to $\sim$5 for the cleaned field). However, if we use too small a match radius ($\lesssim$ 2.5 arcsec), we risk eliminating real matches. At our typical detection levels of $\sim$4–5σ, the rms positional errors at 24μm are $\sim$1.5 arcsec. Additionally, from examination of our HST ACS images (see the Appendix for more information), we discovered that using a matching radius of 4 arcsec could introduce more false detections than anticipated due to the crowded nature of our group-dominated fields. For these reasons, we used the 3 arcsec matching radius. A 3 arcsec matching radius results in $\sim$4.2 incorrectly matched galaxies for the groups and $\sim$2.7 for the cleaned field for all galaxies. If we assume that all of the mis-matched galaxies are detected at 24μm, we would have upper limits that $\lesssim$ 5.6% and $\lesssim$ 6.5% of detected group and field galaxies, respectively, are incorrectly matched.

We also need to keep in mind that we are comparing group and field galaxies en masse, not individually. False detections will affect the groups and field each the same way, and so will not bias our results provided that the number of false detections remains low, which we have already shown to be the case. As such, the matching technique (and match length of 3 arcsec) is sufficient for our purposes.

3. IR Properties of Sample Galaxies

Extreme environments, such as the interior regions of clusters, clearly quench star formation in galaxies and reduce their IR outputs (e.g., Bai et al. 2009). Based on the ages of their dominant stellar populations and distributions of morphologies, galaxies in rich groups and clusters must have a similar evolution, at least at low redshift (Balogh & McGee 2010). This suggests that galaxy transformation occurs in groups as well as in clusters. To test for such behavior, we compare the fractional IR LF in groups with that of field galaxies at intermediate redshifts.

3.1. Methodology

To compare the IR output and SFR of group and field galaxies, we estimated the SFR and total IR luminosity (L_{TIR}) from the 24μm flux densities using the method described by Rieke et al. (2009), who use *Spitzer* data to create a group of luminous star-forming galaxy templates more complete in the near- and mid-IR than previous templates.

Our method for determining SFR and L_{TIR} is only accurate for purely star-forming galaxies. Obscured active galactic nuclei (AGNs) can also emit a significant fraction of their light in the mid-IR. To identify possible AGN contaminants in our sample, we compared our 24μm-detected galaxies with *Chandra* detections. Four of the galaxies in the CNOC2 sample were identified as AGN with clear X-ray detections, though all four were field galaxies outside of our redshift range (i.e. not in our GEEC sample). However, some AGN may be so buried that we are not able to detect them at our current X-ray detection threshold. More importantly, slightly less than half of the groups targeted by MIPS have X-ray coverage, so there may still be some AGN contaminating our sample. Given the few AGN detected with the existing data and in previous studies of AGN activity in groups (Dwarakanath & Nath 2006; Silverman et al. 2009), we expect this number to be small.

To correct for the different redshifts of our group and field galaxies, we used the derived luminosity evolution of IR galaxies from Le Floc'h et al. (2005), who show that IR galaxies as a whole evolve in luminosity as $(1+z)^{3.2}$ from $z \sim 0$ to $z \sim 1.2$. We evolved our group and field galaxy IR luminosities to a fiducial redshift ($z = 0.5$) to remove redshift bias in our sample. This IR luminosity evolution is for all IR galaxies regardless of environment; however, the Le Floc'h et al. (2005) sample (as for most field samples) is expected to be $\sim$50% groups, $\sim$50% true field galaxies, making this model reasonable for our purposes. This conclusion is supported by the lack of significant differences in the field and group fractional luminosity functions (fLFs) as discussed below.

3.2. Results for IR-active Galaxies

3.2.1. IR Luminosities and Star Formation Rates

In Figure 1 we present L_{TIR} (left axis) and SFR (right axis) with respect to redshift for all galaxies in the CNOC2 survey for which we have MIPS 24μm detections. Group galaxies are shown as solid red circles, while field galaxies are open blue circles and the X-ray identified AGN are overplotted as green triangles. The average detection limit for all of our 24μm fields is shown by the solid black curve; the redshift limits of our GEEC group and field sample are denoted by dashed lines ($0.3 \lesssim z \lesssim 0.55$). The group and field IR-active populations do not appear significantly different.

Figure 2 gives us a clearer picture of the group and field populations in terms of L_{TIR}. We plot histograms of the normalized distributions of L_{TIR} (which we will refer to as fLFs from here on) for the group and field galaxies (red filled circles and blue open circles, respectively). The dashed line indicates our 24μm detection limit for all field galaxies, while the dotted line is the detection limit for all group galaxies. The fractions in each bin (y-axis values) are normalized by the number of 24μm-detected galaxies in each environment and corrected for spectroscopic incompleteness as a function of magnitude. Weights were computed using the method outlined in Appendix A of Wilman et al. (2005a), except in this case we do not correct for any radial dependent selection, which tends to overweight galaxies on the outskirts of groups.

We have also corrected for completeness with respect to the 24μm data. We calculated the 24μm incompleteness by estimating the SFR corresponding to the detection limits for all galaxies in each image. We then found the fraction of group and field galaxies (separately) with SFR detection limits below a given SFR; the inverse of this fraction in each bin corresponds to our 24μm completeness weighting. The completeness corrections for the points shown above both of these limits are small: factors of $\lesssim 1.7$ for both the group and field galaxies.

The group and field galaxy fLFs are identical within the error bars up to $\log(L_{TIR}\ (L_\odot)) \sim 12$. The last two bins contain few galaxies, so we cannot compare the bright end with much certainty. The measurements slightly below our detection limit should not be significantly biased given the care to avoid bias in the sample selection (Wilman et al. 2005a) and that the vast majority of the group and field galaxies have detection limits below the indicated limit; therefore, we can say that these data also agree within the error bars with some certainty. Overall, the fLFs suggest that there is little difference between the groups and the field (with respect to L_{TIR}). Given that there are similar numbers of spectroscopically-identified galaxies in the groups and field in this redshift range, even the overall normalization will

be the same. This seems to indicate that the group environment is not responsible for suppressing or enhancing star formation amongst the actively star-forming population. To confirm the apparent similarity of the group and field samples, we performed a two-sample Kolmogorov-Smirnov (K-S) test on the unbinned fLFs (the raw L_{TIR} distributions) in both environments. The K-S test indicated a ∼99% probability that the two distributions can come from the same parent sample. Due to the coupling between L_{TIR} and SFR through L(24μm) (Rieke et al. 2009), the results are the same if we plot SFR instead of L_{TIR}.

To better quantify the two LFs themselves, we fit both with a Schechter function, minimizing χ^2. Log(L^* ($L_\odot$)) for the groups and field, respectively, are 11.9 ± 0.5 and 12.3 ± 0.3, a difference of ∼0.4 dex, though, given the error bars, the two environments are similar. Tran et al. (2009) find the opposite trend: their supergroup L^* is ∼0.4 dex higher than the field. The faint-end slope alpha does not differ significantly between the two environments either. We find alpha to be 2.9 ± 1.1 and 4.3 ± 1.2 for the groups and field, respectively.

Figures 1 and 2, and our statistical analysis of the results, suggest that the group environment does not substantially quench or enhance star formation at intermediate redshifts for the IR luminosities we are studying. Could the environmental effects be more prominent in the larger groups? To test this possibility, we plot the number of group members brighter than M_{B_J} = -20 versus L_{TIR} (luminosity-evolved to z ∼ 0.5) in Figure 3. The open circles are individual galaxies, and the filled red circles show the mean L_{TIR} in three bins for all detected group galaxies with 1σ error bars. For reference, most groups have velocity dispersions less than 500 km s^{-1} while the largest group is ∼740 km s^{-1}([4]). We see no trend in 24μm-detected galaxies with respect to group size, and the differences between the mean IR luminosity values is not significant. Therefore, within the L_{TIR} limit of our sample, group size does not strongly affect the IR luminosity of the member galaxies. This is interesting given that interactions are thought to be a major source of star-formation quenching in groups (given that higher densities are needed for other quenching mechanisms like ram-pressure stripping and strangulation), and the number of galaxies that have experienced past interactions and mergers should be larger in more massive groups, which have more

[4]The group membership determination to the limiting magnitude is complete to the ∼70%–90% level, so variations in the completeness are not large enough to affect the basic result shown in the figure. Ideally, we would compare L_{TIR} directly with group mass determined from the velocity dispersions, but for values below ∼350 km s^{-1} the velocity dispersions can significantly underestimate the group mass (Nolthenius & White 1987). Additionally, for small groups, the orientation angle of the group on the sky may add uncertainty in translating the velocity dispersion to the mass (Plionis & Tovmassian 2004). The velocity dispersions for some of our groups have large formal errors, and a significant fraction of the groups may also not be virialized (e.g., Bai et al. 2009, Hou et al. 2009).

members.

Our results are in agreement with many recent studies of clusters. At similar redshifts to our groups ($0.4 \lesssim z \lesssim 0.8$), Finn et al. (2010) find that clusters have IR LFs very similar to the field. This seems to be true with local clusters, as well (Bai et al. 2006, 2009), indicating that IR-active galaxies in clusters have been recently-accreted and have not yet had time to become affected by the more dense environment of the cluster. Cortese et al. (2008) find that the UV LF of the Coma cluster is indistinguishable from the field; however, they argue that this is due more to color selection effects than environmental processes. We believe that the GEEC R_C selection does not cause significant selection effects, but further study would be needed to determine how this R-band selection might affect our results.

3.2.2. Star Formation with Respect to Mass

While the total IR luminosities and SFRs of the group galaxies do not appear different from the field, there could be trends with stellar mass. The most massive galaxies in dense regions of the local universe, such as cluster cores, are old ellipticals, whereas the most massive field galaxies are blue spirals. What about groups at intermediate redshifts?

The stellar masses used here are presented in McGee et al. (2011), but briefly, we use spectral energy distribution (SED) fitting of all available photometry. The details of the photometry were presented in Balogh et al. (2009) but typically involved K, i, r, g, u, NUV and FUV. We compare this observed photometry to a large grid of model SEDs constructed using the Bruzual & Charlot (2003) stellar population synthesis code and assuming a Chabrier initial mass function. We follow Salim et al (2007) in creating a grid of models that uniformly samples the allowed parameters of formation time, galaxy metallicity, and the two components of the Charlot & Fall (2000) dust model. The star formation history is modeled as an exponentially declining base rate with bursts of star formation randomly distributed in time, which vary in duration and relative strength. We produce model magnitudes by convolving these model SEDs with the observed photometric bandpasses at nine redshifts between 0.25 and 0.6. Finally, we minimize the χ^2 while summing over all the models and taking account of the observed uncertainty on each point. By comparing to other estimates of stellar mass we estimate that 1σ uncertainties are on the order of 0.15 dex.

We investigate SFR with respect to stellar mass in Figures 4 through 6. Figure 4 shows SFR plotted with respect to stellar mass for the group (red filled circles) and field (blue open circles) galaxies. Only galaxies above our 24μm detection limit (dashed line) are shown. Because our sample is only unbiased for $\log(M_*(M_\odot)) \gtrsim 10$, we average the SFRs for each

environment in three mass bins above this limit. These averages are plotted as black filled triangles for the groups and black open triangles for the field. Unlike the previous figures, the field has a different distribution than the groups. Noeske et al. (2007) compare SFR and stellar mass for 24μm-identified "field" galaxies in a similar redshift range ($0.2 \lesssim z \lesssim 0.7$) and find a linear relation between SFR and stellar mass with a slope of $\sim$0.67. They did not distinguish between group and field galaxies, however, so their "field" is a combination of the two environments. We compared our galaxies with theirs by plotting this relation as a solid, black line (with an arbitrary normalization). Our group and field galaxies, combined, seem to echo the Noeske et al. (2007) relation, with the suggestion that galaxies in the field obey a steeper mass–SFR relationship than those in groups (mainly driven by the lack of high-mass galaxies with SFR just above our detection limit in the field, a region populated by group galaxies).

In Figure 5, we plot a "specific SFR function" (SFR M_*^{-1}) in the same manner as Figure 2, though only including galaxies with SFR $\gtrsim 2.7$ $M_\odot$ yr^{-1}. Each histogram has been normalized so that its total is 1. Differences between the group and the field are suggested; a two-sample K-S test reveals that the two distributions have only a 27% probability that they are drawn from the same parent sample. The groups have more IR-active galaxies with less star formation per stellar mass than the field galaxies, as expected given the overall higher masses of the group galaxies. Put another way, for the IR-detected galaxies in the groups, the on-going star formation makes a smaller relative contribution to the stellar mass than for galaxies in more isolated environments. Thus, the average timescale for growth of the stellar mass ($M_*/\dot{M}_*$) is currently smaller in the field than in group galaxies by a factor of $\sim$3. In the past, however, it is possible that this timescale was shorter in the groups given that their galaxies have shifted to higher masses by $z \sim 0.5$.

Figure 6 compares stellar mass and SFR in a slightly different way. The top plot shows the fraction of 24μm-detected field and group galaxies as a function of specific SFR (sSFR) with $\log(M_*(M_\odot)) < 10.5$, labeled as blue dashed and red solid lines, respectively. The lower panel is the same plot except for galaxies with $\log(M_*(M_\odot)) > 10.5$. The histograms in this figure have been normalized in the same manner as Figure 5. We see that group and field galaxies have similar ranges of sSFRs in either mass bin, but the higher-mass galaxies in the field tend to form stars at higher rates (higher-mass group galaxies have lower relative SFRs). A two-sample K-S test results in a $\sim$3% probability that the low-mass ($\log(M_*(M_\odot))$ < 10.5) group and field galaxies come from the same parent sample and a $\sim$89% probability for the high-mass group and field galaxies ($\log(M_*(M_\odot)) > 10.5$). While neither of these cases indicate a 3σ result, it makes sense given Figure 4, which shows a trend of higher-mass group galaxies having significantly lower SFRs as compared with the field. The subtle trends seen in Figures 5 and 6 may be showing the beginning stages of suppression of star formation

in the groups.

In Figure 7, we split our group and field galaxies in terms of their SFRs with respect to stellar mass. The top plot shows the fraction of what we call "low-activity" galaxies (SFR < 2.7 $M_\odot$ yr^{-1}) normalized by the total number of galaxies per mass bin in the groups (red solid line) and field (blue dashed line). The two highest mass bins in the groups house a total of three galaxies, all of which are in groups with 10 or fewer members, so any trend in the number of low-activity, high-mass group galaxies does not appear to be significant. As a result, the group and field galaxies are similar in terms of the fraction of low-activity galaxies for a given stellar mass. The bottom plot shows the fraction of galaxies in each environment with SFR > 10 $M_\odot$ yr^{-1} with the same normalization as the top plot. We do potentially see a stronger difference between the group and field galaxies at these higher SFRs: the groups have galaxies forming stars at this high rate at a variety of masses, while the field galaxies peak at $\log(M_*(M_\odot)) \sim 11$. This may be another indication of a stronger mass–SFR relation in the field than in the groups, though the differences between the group and field galaxies here are of low significance.

We performed a Monte Carlo analysis of the data in the top plot of Figure 7 to estimate whether the overall fraction of low-activity galaxies, at constant stellar mass, is significantly higher for group galaxies. We found the total number of group galaxies per mass bin and randomly selected the same number of galaxies per mass bin from the field, making a fake group sample. We then made the same plot as the top part of Figure 7 using the fake group galaxies: the fraction of fake low-activity galaxies normalized by the total number of galaxies per mass bin. We repeated this 500 times, each time calculating the mean fraction of low-activity galaxies from $10 \lesssim \log(M_*(M_\odot)) \lesssim 11.6$. (Higher masses were not possible given the lack of field galaxies in the highest mass bins.) Because the fraction of low-activity galaxies in the groups and field in this mass range is fairly constant with mass, the average is an accurate way of comparing the fake and real group galaxies. This distribution of fake group averages is plotted as a histogram in Figure 8; it is fit well by a Gaussian (solid curve). The mean of the real groups (real field) is shown as a dashed (dotted) line. The fake groups have consistently low averages as compared with the real groups, though this difference is only significant to a 1σ level. Interestingly, the resampled field (matched in mass to the group population) has a mean low-activity fraction equivalent to the non-resampled field, indicating that the dependence of low-activity fraction on mass within this range is negligible (also evidenced by the lack of a trend in Figure 7).

Another way to describe these results is that, if we use the field mass-SFR relation to determine the expected IR luminosity distributions in groups, we would conclude that the groups are slightly under-luminous because of their higher proportion of high-mass galaxies.

Marcillac et al. (2008) study the environment of $0.7 \lesssim z \lesssim 1.0$ LIRGs and ultraluminous IR galaxies (ULIRGs), and they find that, at similar masses, 32% of all the galaxies in their sample reside in groups, and 32% of their LIRGs and ULIRGs also reside in groups. Where we find a small and barely significant difference, their study indicates none. That is, this reinforces our conclusion that the group environment does not suppress or enhance star formation in the galaxies as a whole. Though we do see indications of suppression in the groups when we compare sSFRs, the difference is subtle and might depend on the low-mass regime where we are incomplete (galaxies with lower SFRs than we were able to detect with MIPS), or other variables.

3.2.3. Morphologies

Another parameter subject to transformation in dense environments is galaxy morphology. Is there any difference in morphology types with respect to star formation between the group and field galaxies? Wilman et al. (2009) report on the visual morphologies of the GEEC groups and field galaxies using high-resolution ACS data. They find that the two environments tend to harbor different types of galaxies: S0 galaxies are more prevalent in groups than in the field at a fixed luminosity, indicating that suppression of star formation and bulge growth have been more common in the group environment. Overall, for galaxies brighter than M_{r_0} = -21, they find that the groups have about 1.5 times the number of E/S0 galaxies as the field (Wilman et al. 2009).

We compared the visual morphologies with our IR SFRs using the Wilman et al. (2009) classifications. Thus, "early-type spirals" (eSp) are galaxies classified as Sa through Sbc (including barred spirals), and "late-type spirals" (lSp) are classified as Sc through Sm (including barred spirals). The fractions of IR-detected galaxies with optical classifications (both groups and the field) are as follows: 13% of ellipticals, 10% of S0s, 60% of eSps, 33% of lSp, 15% of irregulars, 17% of mergers, and 61% of galaxies identified as "peculiar." It is perhaps a surprise that eSps are twice as likely to be detected at 24μm as lSps, but this difference may arise because of the lower masses of the later galaxy types.

These conclusions can be tested with quantitative morphology metrics, such as the Concentration, Asymmetry, Clumpiness method (Abraham et al. 1994, 1996; Conselice et al. 2000, 2003; see also McGee et al. 2008 for other methods). At $z \sim 0.5$, surface brightness dimming might become a problem when identifying spirals, particularly late-types, as the fainter spiral features become indistiguishable from the background. Shi et al. (2009) have shown how to correct concentration and asymmetry (referred to as CA from now on) for the effects of surface brightness dimming to provide unbiased metrics at and above the redshifts

of our groups. We have used their methodology to calculate CA for our sample of field and group galaxies, as shown in Figure 9 (small black dots). In the top plot, the average values (and error bars) for the groups and field galaxies are given by the red square and blue star, respectively. The dashed line is an arbitrary division roughly separating early- and late-type galaxies that we discuss below. Consistent with Wilman et al. (2009), our results indicate a tendency for group galaxies to have, on average, a higher concentration and lower asymmetry (indicative of E and S0 galaxies) than in the field.

Of 144 galaxies detected at 24μm, seven are Es and four are S0s. Three of the galaxies are classified as "peculiar," which means they have been visually identified as either having an interacting neighbor or a morphology slightly disturbed from the given classification, and one galaxy is listed as an S0/Sa (most likely an S0 but also has Sa qualities). Still, it is unusual to find any E or S0 galaxies with SFRs at these levels. To be certain the early-type galaxy detections are robust, we investigated other possibilities for the IR emission.

The first issue concerns our source matching: is it possible that there are nearby (projected) neighbors that are being mis-matched with the E/S0 galaxies? As discussed in the Appendix, inspection of the ACS images shows that a few of the early-type galaxies have close neighbors, making identifying which galaxy in the field of view is responsible for the IR emission difficult. To be conservative, we rejected any early-type galaxies where the IR emission could be coming from another object. After removing these ambiguous E/S0 detections, we were left with four ellipticals and two S0s firmly detected at 24μm. We also double-checked our matching of the 24μm positions with the IRAC 3.6μm coordinates. Four of the six E/S0 galaxies have IRAC coverage, and all of them match the IRAC coordinates within 1.5 arcsec or less. Because we have imposed very stringent requirements to claim a detection, six detected E/S0 galaxies represents a lower limit.

As a double–check on the morphologies, we again plot asymmetry and concentration for all galaxies with CA values (small, black circles) and the six IR-active early-type galaxies (red circles for ellipticals and black triangles for S0s, with filled points indicating a group galaxy and empty points indicating a field galaxy) at the bottom of Figure 9. All six galaxies fall in the "early-type" area of the plot, and they also all fall well under our early-/late-type dashed line. It appears that these six E/S0 galaxies are indeed early-types with bright 24μm emission.

There is one other culprit that could be masquerading as star formation, however: AGNs. Of the six early-type galaxies with confirmed IR emission, only two have X-ray coverage, though neither of them are detected down to $L_X \sim 10^{41}$ erg s^{-1} (Mulchaey et al. in prep). As an additional test for AGNs, we look to the IRAC data. The intersection of the stellar light and the warm/cool dust components produces a dip in the SED at rest-frame

$\sim$5μm for normal star-forming galaxies. Buried AGNs heat the dust to higher temperatures, which "fills in" this dip. If our IR-detected early-type galaxies have similar colors at IRAC wavelengths to the typical galaxies in our sample, then AGNs are probably not contributing significantly to the mid-IR emission. In Figure 10 we plot IRAC [3.6]–[4.5] and [3.6]–[5.8] versus redshift for all galaxies with IRAC coverage in our sample. Most of the galaxies fall into a narrow color range in both plots, indicating that we are probing the Rayleigh–Jeans tail of the stellar bump. If the 24μm emission were dominated by an embedded AGN, these colors would be more positive due to the warm dust filling in the "dip" in the SED, causing the SED to brighten as we move through the IRAC bands. None of the early-type galaxies detected at 24μm (with IRAC coverage) show the signature of an AGN in the IRAC colors.

Two of our six IR-bright early-type galaxies do not have X-ray or complete IRAC coverage. We have enough SED coverage of one of these two to make out some of the stellar bump and the increase in dust emission in the IR, which seems to indicate star formation instead of an AGN, but it is difficult to say with certainty. The other source has too few photometric data points to make any solid conclusion; however, given the lack of AGNs we have found so far in our entire sample, it seems that AGNs are a rarity. While we cannot be certain that these two galaxies do not host AGNs, it seems unlikely.

Thus, even by these stringent tests, we have detected four elliptical and two S0 galaxies at 24μm, none of which have an obvious AGN contribution. Five of these galaxies (three ellipticals and two S0s) are in groups. We cannot tell whether the groups and field are different in this regard at a statistically significant level. However, among the IR-detected group members, $\gtrsim$ 6% are early types. That is, some early-type galaxies in groups were forming stars at significant levels around z $\sim$ 0.5. We can compare this behavior with that of local early-type galaxies using the study of Devereux & Hameed (1997). They extracted IRAS 60μm detections of galaxies in the Nearby Galaxies Catalog (NBGC; Tully 1989), which contains 2367 galaxies within 40 Mpc (H_0 = 75 km s^{-1} Mpc^{-1}). After eliminating ones not covered by IRAS or compromised for other reasons, 2094 remained in this study, of which 1215 were detected by IRAS (including 22% of the 151 ellipticals). We determined the 99th percentile of 60μm luminosity for the E–E/S0 and S0–S0/a categories and converted it to L_{TIR} of 2.4 $\times$ 10^9 L$_\odot$ and 2.3 $\times$ 10^{10} L$_\odot$, respectively. The corresponding SFRs are 0.27 and 2.6 M$_\odot$ yr^{-1} (Rieke et al. 2009) and are indicated in Figure 11 by dashed and dotted lines, respectively. Figure 11 also shows stellar mass versus SFR for all galaxies in our sample detected at 24μm (small black dots), separated by environment, with visual morphologies indicated by a variety of symbols. The SFRs for the two group S0 galaxies are at or just below the 99th percentile for local S0–S0/a galaxies, while the SFRs of all four E galaxies exceed the 99th percentile for local E–E/S0 galaxies by factors of 3–20, an unexpected result given that there are less than 100 early-type group members in our sample.

On a more general note, these measurements imply that not all early-type galaxies are dead at z $\sim$ 0.5; many are still in the process of forming stars, indicating a larger amount of evolution with redshift than previously thought (e.g., Larson 1974; Chiosi & Carraro 2002). While it does appear that there are still some early-type galaxies forming stars in the local universe (Temi et al. 2009), the ubiquity of IR-active early-types in group and field environments remains largely unknown. We do know, however, that star formation in E/S0 galaxies has been decreasing since z $\sim$ 1. Kaviraj et al. (2008) find that star formation in early-type galaxies has decreased by $\sim$50% since z $\sim$ 0.7, and they show that local early-type galaxies, while largely quiescent now, have had spurts of star formation in their recent past. Thus, the enhancement of star-forming activity in early-type galaxies at z $\sim$ 0.5 compared with the present epoch may apply generally for field and group members.

We now discuss the fraction of 24μm-detected galaxies with respect to the full range of morphologies, separated by groups and field. As just discussed, for E/S0 galaxies, 5 out of 75 in groups were detected at 24μm (7%) and 1 out of 22 in the field (5%). eSps behave similarly in the two environments: 29 out of 47 group galaxies were detected (62%) compared with 14 out of 23 (61%) in the field. For lSps, 9 out of 19 (47%) are detected in groups and 4 out of 20 (20%) in the field. Although there is a hint of a larger incidence of late-type galaxies with high SFRs detected in our group sample, there are no differences at a significant level.

4. DISCUSSION

There is strong agreement that the dense environments in the cores of clusters do have a large effect on their member galaxies in terms of star formation. Marcillac et al. (2007), Patel et al. (2009), and Koyama et al. (2010) show that the densest regions of the clusters RXJ 1716.4+6708 and RXJ 0152.7-1357 strongly suppress star formation. Using the CNOC1 cluster galaxy sample ($0.2 \lesssim z \lesssim 0.55$), Balogh et al. (2000) find that the mean galaxy SFR decreases with decreasing radius from the center of the cluster, and Ellingson et al. (2001) shows a decrease in the fraction of blue and emission-line galaxies and an increase in the fraction of ellipticals as one approaches the cluster core. Similarly, for the more distant cluster MS 1054-03 (z $\sim$ 0.8), Bai et al. (2007) observed that star formation in member galaxies near the core was substantially suppressed; Vulcani et al. (2010) find the same suppression in cluster galaxies from $0.4 \lesssim z \lesssim 0.8$ as compared with the field, though the reduction in SFR was more modest in those clusters. Locally ($z \lesssim 0.3$), we continue to see star-formation quenched or suppressed near cluster cores: Haines et al. (2009) find suppression for star-forming cluster galaxies (defined by $L_{IR} > 10^{10}$ $L_\odot$), as do Bai et al. (2006, 2009), who report that star-forming galaxies (defined by SFR $\gtrsim 0.2$ $M_\odot$ yr^{-1}) are much less likely

to be found in the cores of local clusters Coma and A3266. Biviano & Katgert (2004) use kinematics of different cluster galaxy morphologies to show that lSps are more likely to be found at higher distances from the core.

Although the SFR suppression in cluster cores is clearly established, work to-date has not reached a firm conclusion about the comparison of group galaxies with those in the field and in clusters with respect to the IR regime. Wilman et al. (2008) find, from 8μm measurements of a subset of the GEEC sample, that the SFR is significantly suppressed in groups as compared with the field at z $\sim$ 0.4. Bai et al. (2010) use 24μm observations to show that local groups have somewhat suppressed SFRs compared with the field, and somewhat elevated ones compared with clusters (though they have a lower SFR limit than our study). At higher redshifts, Marcillac et al. (2008) use a large sample of galaxies in the Extended Groth Strip to find that LIRGs and ULIRGs measured at 24μm do not preferentially exist in higher-density environments (including groups) at z $\sim$ 0.9. Tran et al. (2009) use 24μm data to find a substantially (four times) higher incidence of active star-forming galaxies in groups compared with clusters at z $\sim$ 0.37. They also find that the groups and field are similar in this regard for their luminosity-limited sample. Patel et al. (2009) use 24μm measurements to find a progressive suppression of the SFR by an order of magnitude from the field to cluster core densities.

Other recent studies in optical bands show suppression of star formation in groups due to different mechanisms. Peng et al. (2010) and Kovač et al. (2010) use Sloan Digital Sky Survey and zCOSMOS galaxies at a variety of redshifts (up to z $\sim$ 1) and environments to show that the effects of environment on individual galaxies are separate from the evolution and quenching with increasing galaxy mass. This "mass quenching" is the dominant effect at high galaxy masses ($M_* \gtrsim 10^{10.2}$ $M_\odot$), while other effects, like environmental quenching, dominate for low-mass and satellite galaxies ($M_* \lesssim 10^{10}$ $M_\odot$; Peng et al. 2010). As mentioned previously, Tran et al. (2009) find comparable fractions of star-forming galaxies in their supergroup and the field for a luminosity-limited sample, but their mass-selected sample shows that the supergroup has about half the fraction of star-forming galaxies as the field.

In light of the uncertainties in the effects of groups on the SFRs as reflected in the *Spitzer* 8 and 24μm data, we have carried out a thorough study of the CNOC2 groups at $0.3 < z < 0.55$, which are exceptionally well-characterized and have substantial amounts of ancillary data. The large sizes of this group sample and of the accompanying field sample also allow reasonably good statistics for our conclusions. We find that the incidence of 24μm emission is virtually the same in these groups as in the field. This result agrees well with that of Tran et al. (2009) for their luminosity-selected supergroup at z = 0.37 but has higher statistical weight because our field sample is significantly larger. This agreement is

interesting because Tran et al. (2009) studied super-groups with large velocity dispersions and significant X-ray luminosities, while our groups generally have lower velocity dispersions and no X-ray emission.

This similarity of IR properties appears to hold in detail, both in the forms of the fLFs and as characterized by L^*. The overall fLFs for groups and field are consistent with being drawn from the same distribution. Tran et al. (2009) found that L^* for their field sample was ~ 0.4 dex lower than for their groups. To look for this effect, we used our fLF Schechter function fits to determine L^* for our groups. L^* for our field is marginally larger (again $\sim$0.4 dex) than the groups, though given the error bars on the values of L^*, the field and group L^* are comparable. It is possible that the difference between the two studies arises from the different environments—one large group-like structure for Tran et al. (2009) versus our individual, smaller groups. However, given the statistical significance of the two studies, it is plausible that there is no significant overall difference in L^* between the two environments. This emphasizes the lack of any strong dependence of group member properties on the size or mass of the group (Wilman et al. 2005b; this work).

The IR properties of our group and field galaxies appear to be contrary to the shift in the distribution of galaxy morphologies toward early-types in groups (McGee et al. 2008; Wilman et al. 2009), which we confirm with a form of CA analysis. In part, this apparent contradiction can be explained by the presence of a number of E/S0 galaxies that are detected at 24μm; this IR activity appears to arise from elevated levels of star formation as compared with local E/S0 galaxies (as also found by Tran et al. (2009)). However, this behavior has also been seen at similar redshifts in field early-type galaxies (e.g., van der Wel et al. 2007; Pérez-González et al. 2008). Along with a higher population of E/S0 galaxies, the groups also have larger overall numbers of massive, eSps. These galaxies contribute significantly to the numbers of IR-detected group members and to the group LF. Tran et al. (2009) find a similar result for their super-group: that an excess population (compared with the field) of spirals fills in the dearth of star formation that would otherwise exist because of the larger proportion of early-type galaxies. A minor difference is that the Tran et al. (2009) group sample is rich in relatively low-mass star-forming spirals compared with those in our groups.

An interesting observation is that there are only two galaxies total in our group and field sample that can be classified as ULIRGs ($12 \lesssim \log(L_{TIR}\ (L_\odot)) \lesssim 13$). Le Floc'h et al. (2005) showed that ULIRGs make up only $\sim$10% of the IR population at $z \sim 0.7$, which roughly means, at the redshifts we are studying here, we should expect to see 4–12 ULIRGs. While the errors on this estimate are almost certainly large enough to encompass our two ULIRGs, it is still odd that our sample lies at the low end of the expected range. If galaxies in groups have higher propensities for mergers or low-velocity encounters, we might expect

to see more of these high-L_{TIR} galaxies in the groups, if not overall. Geach et al. (2009) suggest that such encounters could be fueling the growth of galactic bulges, which explains the larger fraction of Sa through E galaxies in the groups. If we do not see massive amounts of star formation in the groups—or, in this case, neither the groups nor the field—then either a process common to both group and field galaxies is responsible for the bulge formation or star formation from mergers and low-velocity encounters is short enough to not show significant IR emission in individual galaxies.

Because mass has been shown to have significant association with suppressing star formation, we also made a quantitative test of the overall similarity of group and field members of similar mass. The ratio of low-activity star forming galaxies (i.e., those with SFR < 2.7 $M_\odot$ yr^{-1}) to the total number of galaxies with $M_* > 10^{10}$ $M_\odot$ is 0.69. We synthesized this result from field galaxies in a Monte Carlo calculation, drawing randomly from a field sample matched in mass. The synthesized distribution is Gaussian and has its maximum probability at a fraction of 0.66, with a range at $\pm 1\sigma$ from 0.62 to 0.70. That is, there is only marginal evidence (1σ) for a change in incidence of high levels of star formation in galaxies of the same mass in groups versus the field, and any such change is limited to be no more than a 10% effect (at 1σ).

All of these results are consistent with the hypothesis that the difference between the group and field populations is confined largely to their differing mass functions. For a given mass and morphological type, there is no statistically significant suppression or enhancement of star formation in individual group galaxies in the intermediate stellar mass range of 10^{10} to 2×10^{11} $M_\odot$. However, groups have begun to build massive galaxies with lower sSFRs as typical for their relatively-early types. The shifts toward lower sSFRs and toward higher masses tend to cancel each other, leading to similar infrared fLFs.

We must remind ourselves, however, that we are only probing the brightest star-forming galaxies at these redshifts; galaxies with SFRs below our detection limit could be more affected by the group environment, resulting in a lower fraction of star-forming galaxies in the groups (Peng et al. 2010). Locally, the fraction of IR-active galaxies in the two environments differs by $\sim$30% (more star-forming galaxies in the field) for galaxies with SFRs $\gtrsim 0.1$ $M_\odot$ yr^{-1}, a much lower detection limit than our sample (Bai et al. 2010). Other group studies have found environmental dependence of the fractions of star-forming group and field galaxies at fixed luminosity or stellar mass using different indicators (Wilman et al. 2005a, 2008; Balogh et al. 2007, 2009).

These differences suggest that groups are indeed an intermediate stage between the field and clusters. Our groups contain fractions of E and S0 galaxies at levels comparable to clusters (Wilman et al. 2009), and the mass distribution of group galaxies tends to extend

higher than that of field galaxies, as confirmed with a more detailed inspection of the group and field galaxy masses. Despite these differences, the overall IR activity in groups seems to indicate a lack of suppression or enhancement of star formation as compared with the field: the fractions of star-forming galaxies (SFR > 2.7 $M_\odot$ yr^{-1}) are comparable in the groups and field, and the fLFs are nearly identical. Individual galaxies of similar mass and morphology appear to have virtually identical infrared properties in the two environments. Thus, the group environment affects the masses and morphologies of galaxies, and their star forming properties change consistent with these effects. However, any additional changes in star forming properties are, at best, subtle, at least for SFR > 2.7 $M_\odot$ yr^{-1}, indicating that the level of star formation is driven primarily by galaxy mass, itself a function of environment. In other words, star-forming activity in individual galaxies is only indirectly related to the group versus field environment but is linked more strongly to the overall change in galaxy masses and morphologies. The higher L^* for the supergroup of Tran et al. (2009) may indicate an enhancement of star formation that is environmentally-dependent, but they find that mass more strongly affects star formation. Apparently, the assumed increased rate of galaxy-galaxy interactions in groups either does not affect the star formation significantly, or strong interaction-driven star formation occurs in environments other than the groups we studied here.

The outskirts of clusters are a probable alternative location for galaxy processing, as shown by the higher fractions of IR-bright galaxies in group and field galaxies than the outskirts of the Coma and A3266 clusters (Bai et al. 2010). Additional studies of groups and clusters at a variety of redshifts, preferably to lower SFR limits, are needed to further disentangle the effects of these moderately-dense environments on the star formation, mass, and morphology of their member galaxies.

5. CONCLUSIONS

We have observed 26 galaxy groups and accompanying field galaxies with deep MIPS photometry and used 24μm flux densities to estimate the total IR luminosities and SFRs of galaxies in both environments. We find that on an individual basis, group and field galaxies of similar mass and morphology do not differ significantly in terms of their SFRs, and the amount of star formation does not depend on the richness of the groups. However, the groups have systematically lower sSFRs and a higher incidence of massive early-type galaxies, more reminiscent of clusters than the field. We discovered that some of these E and S0 galaxies, as well as a large contingent of massive early spirals, are still forming stars at significant levels. These galaxies may explain why the fLFs of the groups and field are nearly identical despite

the overall decrease in star-forming activity in the groups. The group environment affects galaxy SFRs primarily through the shift toward higher masses, with an accompanying trend toward earlier types and reduced sSFRs. These high-mass, early-type galaxies, along with IR luminosities comparable to the field, put groups in between the field and clusters in terms of overall galaxy properties.

We thank Michael Balogh and Ann Zabludoff for helpful input, the referee for his/her comments and suggestions, and the CNOC2 team for access to their unpublished data. LCP acknowledges financial support from an NSERC Discovery grant. We thank NASA for financial support through contract 1255094 from Caltech/JPL to the University of Arizona. This work is based on observations made with the *Spitzer Space Telescope*, which is operated by the Jet Propulsion Laboratory, the California Institute of Technology, and NASA.

REFERENCES

Abraham, R. G., Valdes, F., Yee, H. K. C., & van den Bergh, S. 1994, ApJ, 432, 75

Abraham, R. G., van den Bergh, S., Glazebrook, K., Ellis, R. S., Santiago, B. X., Surma, P., & Griffiths, R. E. 1996, ApJS, 107, 1

Andreon, S., Willis, J., Quintana, H., Valtchanov, I., Pierre, M., & Pacaud, F. 2004, MNRAS, 353, 353

Bai, L., Rieke, G. H., Rieke, M. J., Hinz, J. L., Kelly, D. M., & Blaylock, M. 2006, ApJ, 639, 827

Bai, L., et al. 2007, ApJ, 664, 181

Bai, L., Rieke, G. H., Rieke, M. J., Christlein, D., & Zabludoff, A. I. 2009, ApJ, 693, 1840

Bai, L., Rasmussen, J., Mulchaey, J. S., Dariush, A., Raychaudhury, S., & Ponman, T. J. 2010, ApJ, 713, 637

Balogh, M. L. & McGee, S. L. 2010, MNRAS, 402, 59

Balogh, M. L., Morris, S. L., Yee, H. K. C., Carlberg, R. G., & Ellingson, E. 1997, ApJ, 488, 75

Balogh, M. L., Morris, S. L., Yee, H. K. C., Carlberg, R. G., & Ellingson, E. 1999, ApJ, 527, 54

Balogh, M. L., Navarro, J. F., & Morris, S. L. 2000, ApJ, 540, 113

Balogh, M. L., et al. 2004, MNRAS, 348, 1355

Balogh, M. L., et al. 2007, MNRAS, 374, 1169

Balogh, M. L., et al. 2009, MNRAS, 398, 754

Biviano, A. & Katgert, P. 2004, A&A, 424, 779

Bower, R. G., Benson, A. J., Malbon, R., Helly, J. C., Frenk, C. S., Baugh, C. M., Cole, S., & Lacey, C. G. 2006, MNRAS, 370, 645

Bruzual, G. & Charlot, S. 2003, MNRAS, 344, 1000

Butcher, H. & Oemler, A., Jr. 1978, ApJ, 219, 18

Carlberg, R. G., Yee, H. K. C., Morris, S. L., Lin, H., Hall, P. B., Patton, D. R., Sawicki, M., & Shepherd, C. W. 2001a, ApJ, 552, 427

Carlberg, R. G., Yee, H. K. C., Morris, S. L., Lin, H., Hall, P. B., Patton, D. R., Sawicki, M., & Shepherd, C. W. 2001b, ApJ, 563, 736

Charlot, S. & Fall, S. M. 2000, ApJ, 539, 718

Chiosi, C. & Carraro, G. 2002, MNRAS, 335, 335

Conselice, C. J., Bershady, M. A., & Jangren, A. 2000, ApJ,529, 886

Conselice, C. J., Bershady, M. A., Dickinson, M., & Papovich, C. 2003, AJ, 126, 1183

Cooper, M. C., et al. 2007, MNRAS, 376, 1445

Cortese, L., Gavazzi, G., & Boselli, A. 2008, MNRAS, 390, 1282

Cucciati, O., et al. 2010, A&A, 524, 2

Devereux, N. A. & Hameed, S. 1997, AJ, 113, 599

Dressler, A. 1980, ApJ, 236, 351

Dressler, A., Rigby, J. R., Oemler, A., Fritz, J., Poggianti, B. M., Rieke, G. H., & Bai, L. 2009, ApJ, 693, 140

Dwarakanath, K. S. & Nath, B. B. 2006, ApJ, 653, L9

Eke, V., et al. 2004, MNRAS, 348, 866

Ellingson, E., Lin, H., Yee, H. K. C., & Carlberg, R. G. 2001, ApJ, 547, 609

Finn, R. A., et al. 2010, ApJ, 720, 87

Finoguenov, A., et al. 2009, ApJ, 704, 764

Geach, J. E., Smail, I., Moran, S. M., Treu, T., & Ellis, R. S. 2009, ApJ, 691, 783

Geller, M. & Huchra, J. 1983, ApJS, 52, 61

Gerke, B. F., et al. 2007, MNRAS, 376, 1425

Gilbank, D. G., Baldry, I. K., Balogh, M. L., Glazebrook, K., & Bower, R. G. 2010, MNRAS, 405, 2594

Gordon, K. D., et al. 2007, PASP, 119, 1019

Gunn, J. & Gott, J. 1972, ApJ, 176, 1

Haines, C. P., et al. 2009, ApJ, 704, 126

Hashimoto, Y., Oemler, A., Jr., Lin, H., & Tucker, D. L. 1998, ApJ, 499, 589

Henriksen, M. & Byrd, G. 1996, ApJ, 459, 82

Hou, A., Parker, L. C., Harris, W. E., & Wilman, D. J. 2009, ApJ, 702, 1199

Iovino, A., et al. 2010, A&A, 509, 40

Johnson, K. E., Hibbard, J. E., Gallagher, S. C., Charlton, J. C., Hornschemeier, A. E., Jarrett, T. H., & Reines, J. A. 2007, AJ, 134, 1522

Just, D., Zaritsky, D., Sand, D. J., Desai, V., & Rudnick, G. 2010, ApJ, 711, 192

Kaviraj, S., et al. 2008, MNRAS, 388, 67

Kaviraj, S., Devriendt, J. E. G., Ferreras, I., Yi, S. K., & Silk, J. 2009, A&A, 503, 445

Kawata, D. & Mulchaey, J. S. 2008, ApJ, 672, 103

Kennicutt, R. C. 1983, ApJ, 272, 54

Kinney, J. D. P., van Gorkom, J. H., & Vollmer, B. 2004, AJ, 127, 3361

Kovač, K., et al. 2010, ApJ, 718, 86

Koyama, Y., Kodama, T., Shimasaku, K., Hayashi, M., Okamura, S., Tanaka, I., & Tokoku, C. 2010, MNRAS, 403, 1611

Larson, R. 1974, MNRAS, 166, 585

Larson, R., et al. 1980, ApJ, 237, 692

Le Floc'h, E., et al. 2005, ApJ, 632, 169

Lin, H., Yee, H. K. C., Carlberg, R. G., Morris, S. L., Sawicki, M., Patton, D., Wirth, G., & Shepherd, C. W. 1999, ApJ, 518, 533

Loh, Y-S., Ellingson, E., Yee, H. K. C., Gilbank, D. G., Gladders, M. D., & Barrientos, L. F. 2008, ApJ, 680, 214

Marcillac, D., Rigby, J. R., Rieke, G. H., & Kelly, D. M. 2007, ApJ, 654, 825

Marcillac, D., et al. 2008, ApJ, 675, 1156

Martig, M., Bournaud, F., Teyssier, R., & Dekel, A. 2009, ApJ, 707, 250

McCarthy, I. G., Frenk, C. S., Font, A. S., Lacey, C. G., Bower, R. G., Mitchell, N. L., Balogh, M. L., & Theuns, T. 2008, MNRAS, 383, 593

McGee, S. L., Balogh, M. L., Henderson, R. D. E., Wilman, D. J., Bower, R. G., Mulchaey, J. S., & Oemler, A., Jr. 2008, MNRAS, 387, 1605

McGee, S. L., Balogh, M. L., Bower, R. G., Font, A. S.,& McCarthy, I. G. 2009, MNRAS, 400, 937

McGee, S. L., et al. 2011, MNRAS, 413, 996

Moustakas, J., Kennicutt, R. C., Jr., & Tremonti, C. A. 2006, ApJ, 642, 775

Mulchaey, J., et al. (in prep)

Noeske, K. G., et al. 2007, ApJ, 660, L43

Nolthenius, R. & White, S. D. M. 1987, MNRAS, 235, 505

Patel, S. G., Holden, B. P., Kelson, D. D., Illingworth, G. D., & Franx, M. 2009, ApJ, 705, L67

Peng, Y.-j., et al. 2010, ApJ, 721, 193

Pérez-González, P. G., Trujillo, I., Barro, G., Gallego, J., Zamorano, J., & Conselice, C. J. 2008, ApJ, 687, 50

Plionis, M. & Tovmassian, H. M. 2004, A&A, 416, 441

Poggianti, B. M., et al. 2006, ApJ, 642, 188

Postman, M. & Geller M. 1984, ApJ, 281, 95

Rieke, G. H., et al. 2004, ApJS, 154, 25

Rieke, G. H., Alonso-Herrero, A., Weiner, B. J., Pérez-Gonzáles, P. G., Blaylock, M., Donley, J. L., & Marcillac, D. 2009, ApJ, 692, 556

Rujopakarn, W., et al. 2010, ApJ, 718, 1171

Salim, S., et al. 2007, ApJS, 173, 267

Shi, Y., Rieke, G. H., Lotz, J., & Pérez-Gonzáles, P. G. 2009, ApJ, 697, 1764

Silverman, J. D., et al. 2009, ApJ, 695, 171

Simard, L., et al. 2009, A&A, 508, 1141

Temi, P., Brighenti, F., & Mathews, W. G. 2009, ApJ, 707, 890

Tran, K.-V. H., Saintonge, A., Moustakas, J., Bai, L., Gonzalez, A. H., Holden, B. P., Zaritsky, D., & Kautsch, S. J. 2009, ApJ, 705, 809

Tully, R. B. 1989, Nearby Galaxies Catalog (Cambridge: Cambridge Univ. Press)

van der Wel, A., Franx, M., Illingworth, G. D., & van Dokkum, P. G. 2007, ApJ, 666, 863

Vulcani, B., Poggianti, B. M., Finn, R. A., Rudnick, G., Desai, V., & Bamford, S. 2010, ApJ, 710, L1

Wilman, D. J., Balogh, M. L., Bower, R. G.,Mulchaey, J. S., Oemler, A., Jr., Carlberg, R. G., Morris, S. L., & Whitaker, R. J. 2005a, MNRAS, 358, 71

Wilman, D. J., et al. 2005b, MNRAS, 358, 88

Wilman, D. J., et al. 2008, ApJ, 680, 1009

Wilman, D. J., et al. 2009, ApJ, 692, 298

Yee, H. K. C., et al. 2000, ApJS, 129, 475

Zabludoff, A. I. & Mulchaey, J. S. 1998, ApJ, 496, 39

Zabludoff, A. I. & Mulchaey, J. S. 2000, ApJ, 539, 136

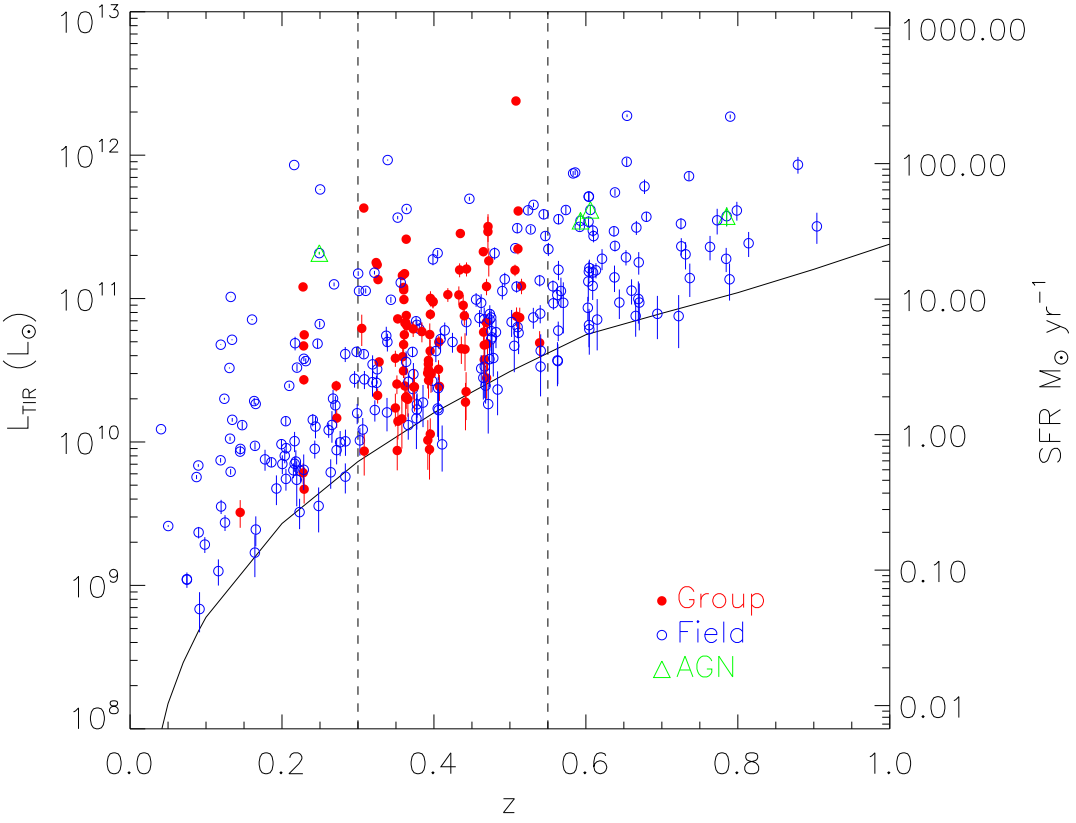

Fig. 1.— L_{TIR} and SFR versus redshift for all galaxies detected at 24μm. The red filled circles are group members, the open blue circles are field galaxies, and the overplotted green triangles are X-ray-detected AGNs. The dashed lines indicate the redshift range of our group and field sample ($0.3 \lesssim z \lesssim 0.55$). The solid line indicates the average 24μm 3σ detection limit for our observations.

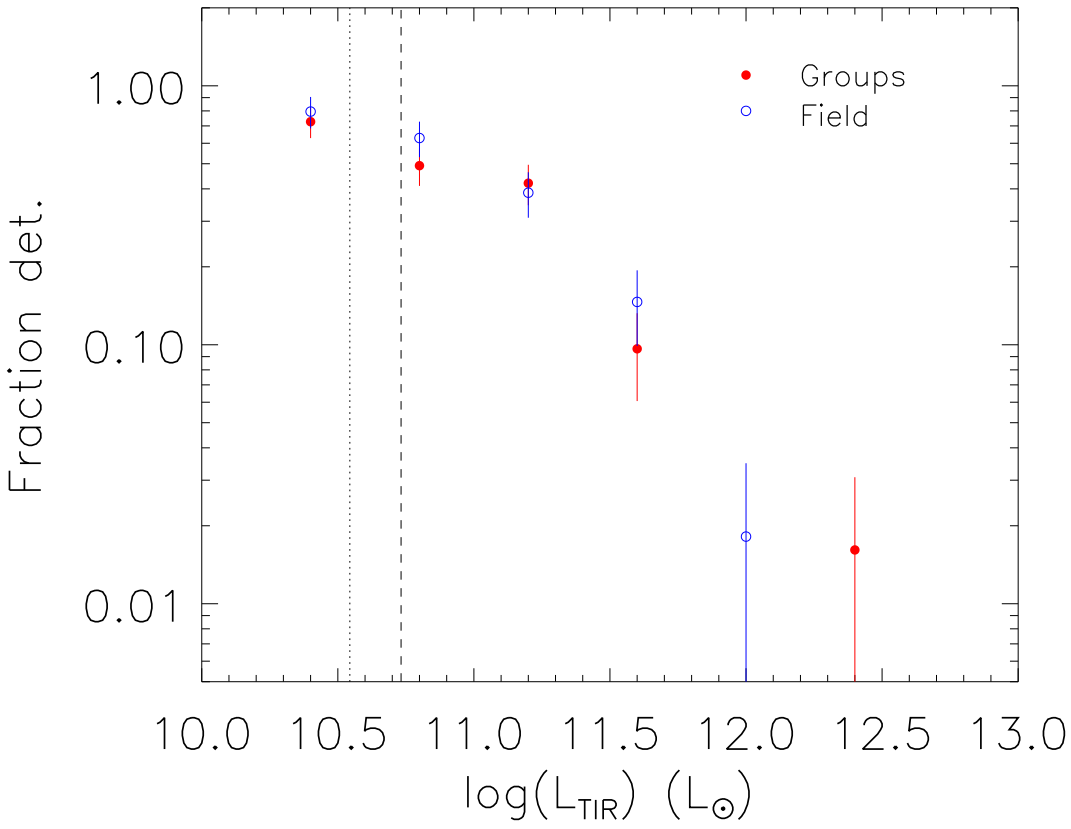

Fig. 2.— L_{TIR} histograms (what we refer to as fractional luminosity functions, fLFs) for the groups (red filled circles) and field galaxies (blue open circles) with Poisson errors. The galaxies included are those detected at 24μm in the redshift range $0.3 \lesssim z \lesssim 0.55$. Each fLF is corrected for spectroscopic and 24μm completeness and has been normalized by the number of IR-detected galaxies in each environment. The vertical dashed line is the detection limit for the field galaxies; the vertical dotted line is the detection limit for all the group galaxies. Up to $\log(L_{TIR}(L_\odot)) \sim 12$, the group and field fLFs are almost identical, given the error bars. The data for the group and field galaxies below the detection limits are also in agreement, though there will be some bias as the group and field galaxies are not equally complete. Above $\log(L_{TIR}(L_\odot)) \sim 12$, we are limited by low number statistics, as there are only a couple group and field galaxies at these luminosities.

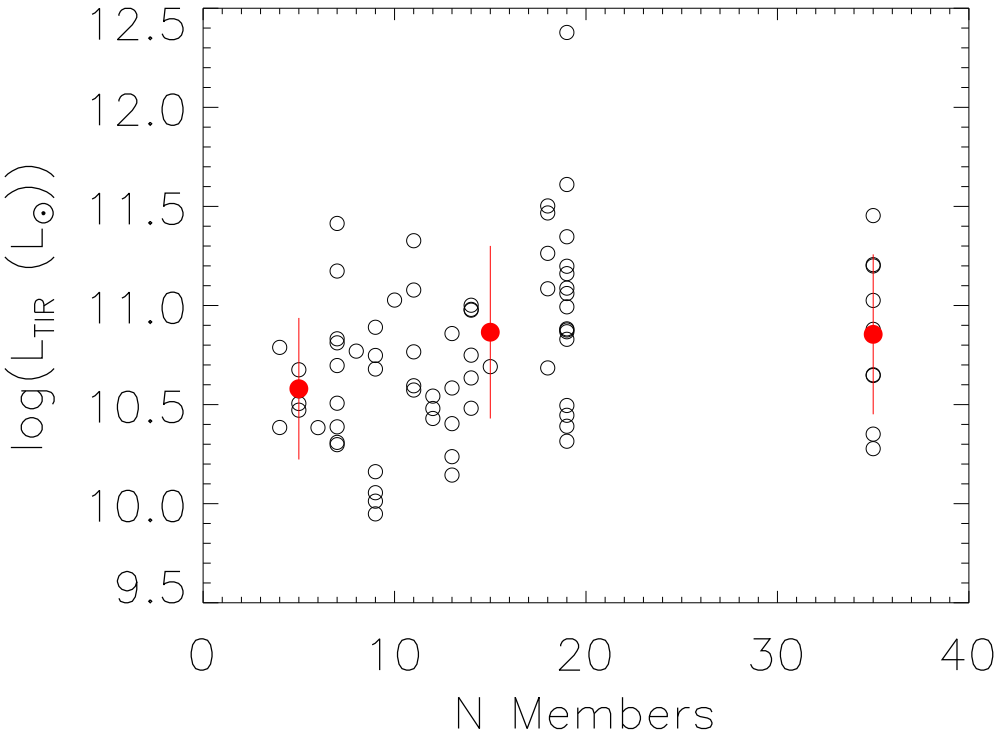

Fig. 3.— L_{TIR} of group galaxies detected at 24μm (luminosity-evolved to z $\sim$ 0.5) versus the total number of members in each group brighter than M_{B_J} = -20. The open black circles are individual galaxies; the red filled circles are the mean L_{TIR} and 1σ error bars for groups in three different bins. The total IR luminosity for individual group galaxies does not depend on the size of the group. In other words, we see no trend in star-formation levels with group richness.

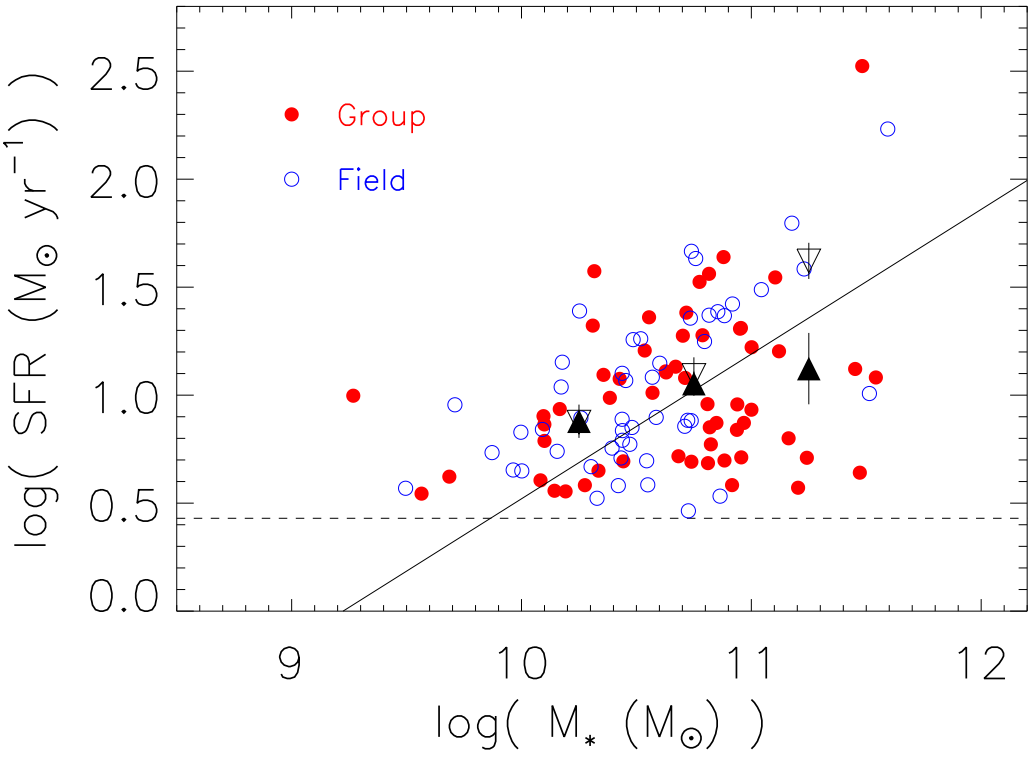

Fig. 4.— Stellar mass versus SFR for IR-detected galaxies in groups (red filled circles) and the field (blue open circles). We only show galaxies above our 24μm detection limit, which is shown by the dashed line. The black filled triangles (black open triangles) are the mean SFR for the groups (field) in three mass bins above $\log(M_*(M_\odot)) = 10$. The field and group galaxies have different distributions. The solid line represents the trend found by Noeske et al. (2007) for 24μm identified "field" galaxies at $0.2 \lesssim z \lesssim 0.7$ (plotted here at an arbitrary normalization). Because Noeske et al. (2007) did not distinguish between group and field galaxies, their trend is likely a combination of the two environments.

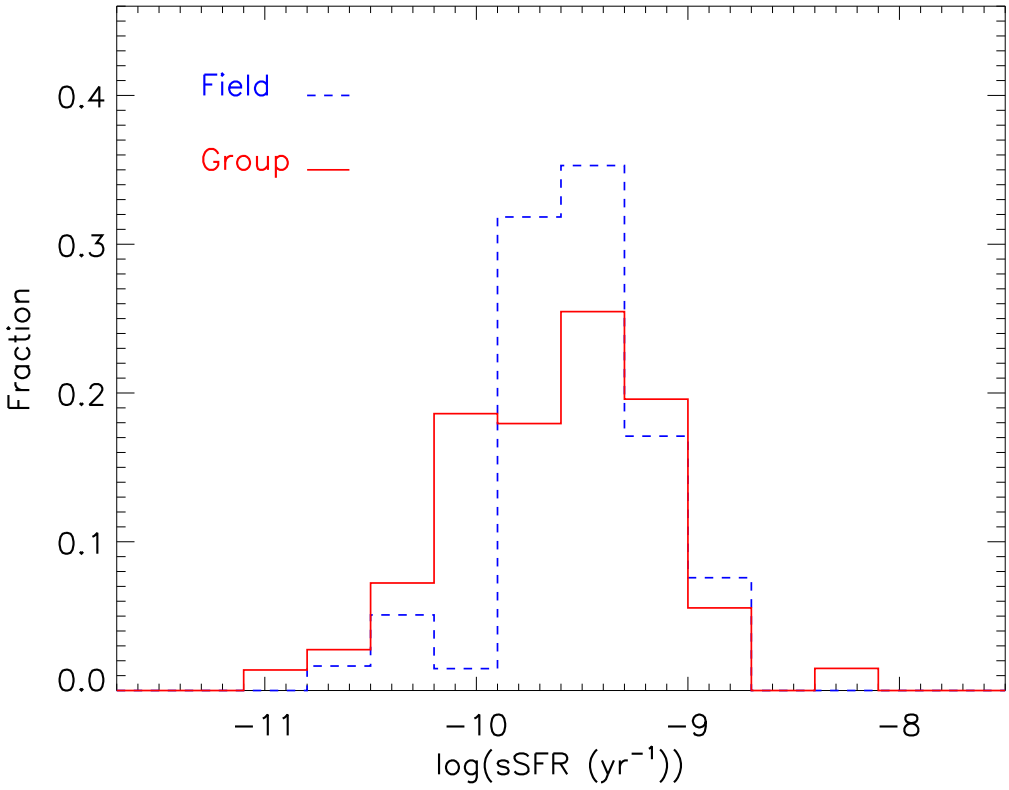

Fig. 5.— Histograms of specific star formation rate (SFR M_*^{-1}) for IR-detected galaxies (SFR $\gtrsim$ 2.7) in groups (red solid line) and the field (blue dashed line), all corrected for spectroscopic and 24μm incompleteness. Each histogram has been normalized so its total value is 1. The groups have more galaxies at higher masses than their field counterparts, resulting in lower specific SFRs for the groups. This difference is not highly significant, however: a two-dimensional KS test results in a 27% probability that these two data sets come from the same distribution.

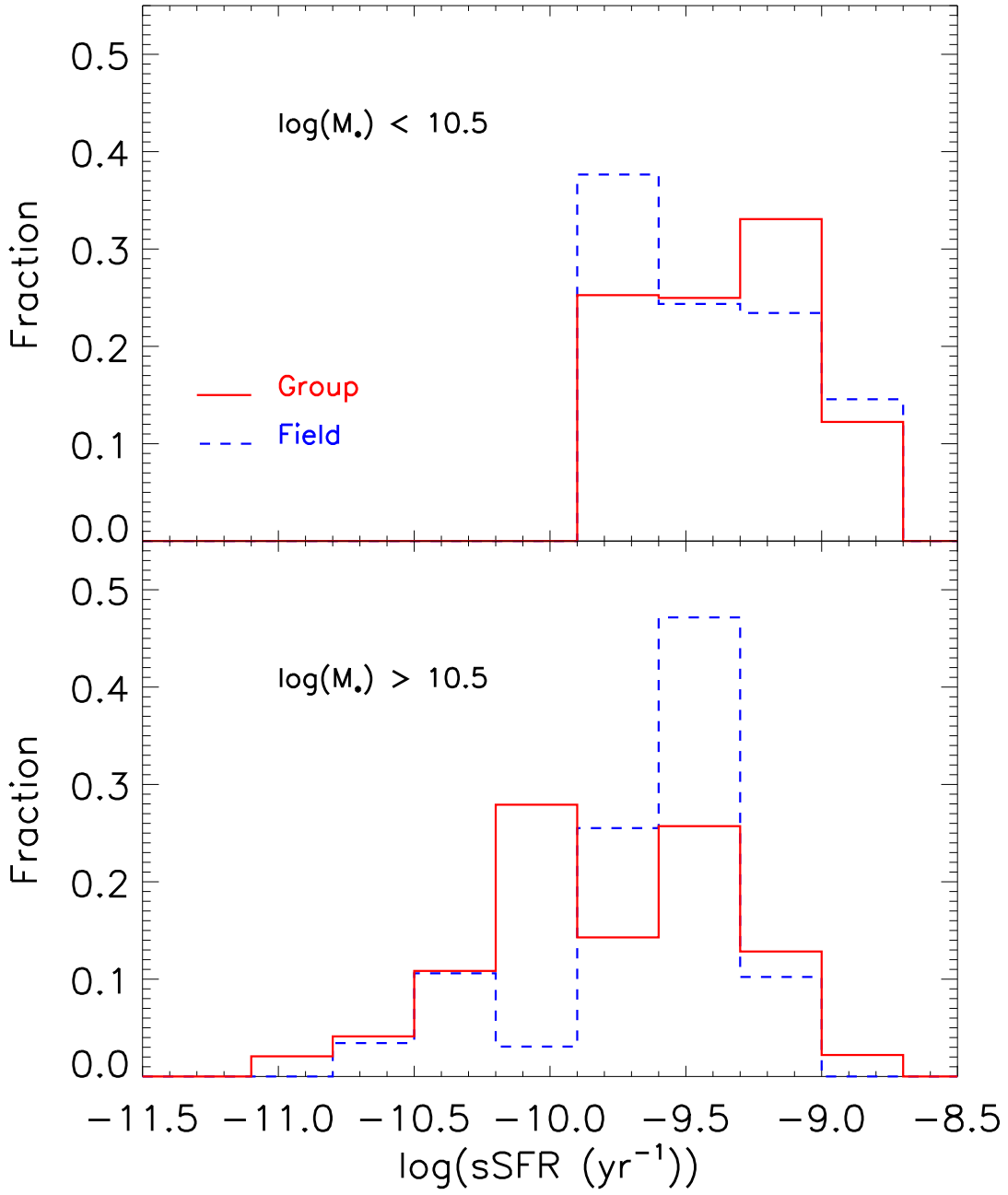

Fig. 6.— Histograms of specific SFR for the field and group galaxies with $\log(M_* (M_\odot)) < 10.5$ (top plot) and > 10.5 (bottom plot), with the same normalization and completeness corrections as the previous figure. While the ranges of sSFRs for both environments are similar, we can see a weak trend whereby massive field galaxies have higher sSFRs than the groups. This same trend was evident in Figure 4, where we can see that the groups tend to have more massive galaxies with lower SFRs than the field. A two-sample K–S test comparing the high-mass group and field galaxies results in a ∼3% probability that the two populations come from the same distribution, and the low-mass group and field galaxies have an 89% probability of coming from the same distribution.

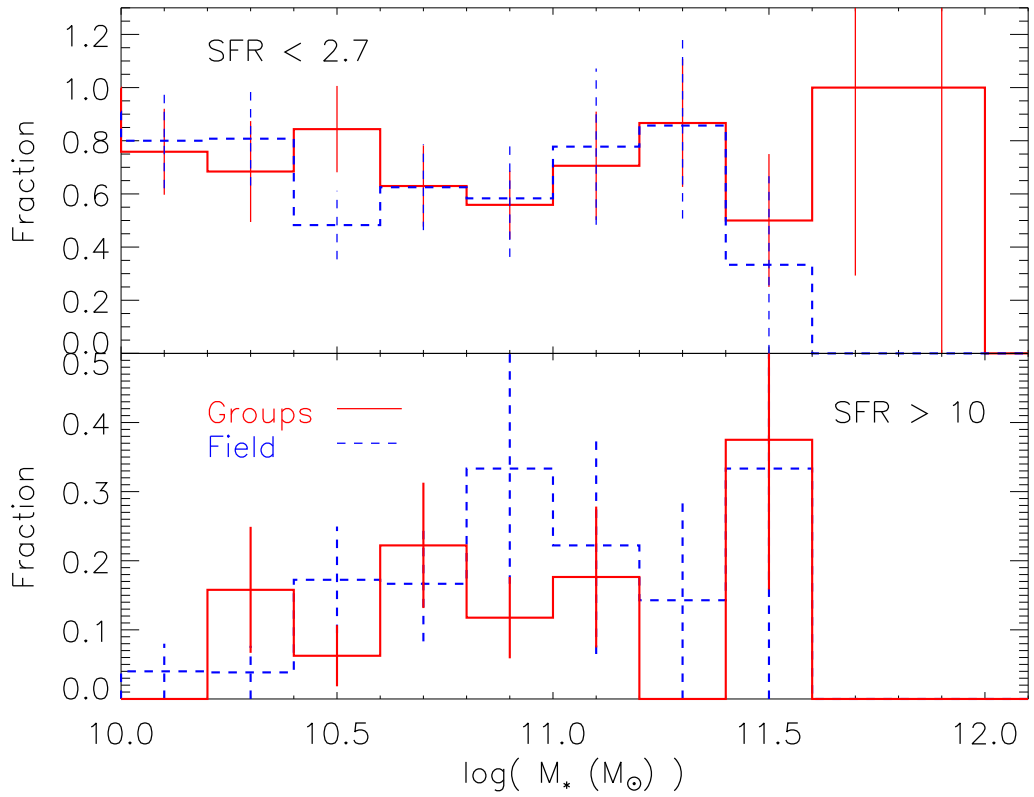

Fig. 7.— Fractions of low- and high-activity galaxies with respect to environment. The top plot shows the fraction of galaxies with SFR < 2.7 $M_\odot$ yr^{-1} normalized by the total number of galaxies in each environment, respectively, per mass bin. For stellar masses below ∼11.5, the groups and the field are nearly identical; above this limit, however, the groups have a few massive, low-activity galaxies while the field has none. (This is not significant, as there are only three galaxies in the two highest mass bins for the groups.) The bottom plot shows the fractions of galaxies with SFR > 10 $M_\odot$ yr^{-1} for each environment, respectively. We see a stronger difference between the group and field galaxies here than in the top plot: the groups have galaxies forming stars at this high rate at a variety of masses, while the field galaxies peak at $\log(M_*(M_\odot)) \sim 11$. This may be another indication of a stronger mass-SFR relation in the field than the group galaxies, though the significance is small.

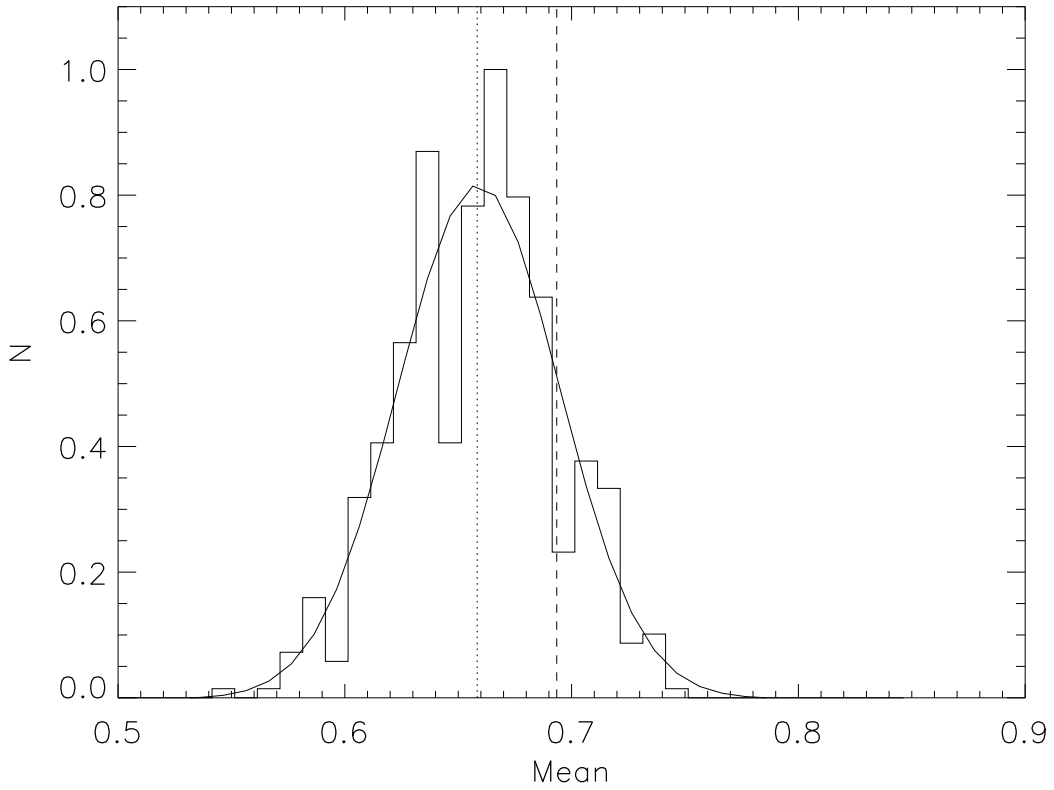

Fig. 8.— Quantitative assessment of the top plot in Figure 7 (see the text for a more specific explanation). We created fake group samples from the field and calculated the average fraction of low-activity galaxies from $10 \lesssim \log(M_*(M_\odot)) \lesssim 11.6$. The histogram shows the distribution of these averages for 500 fake group samples. The dashed (dotted) line is the average fraction of low-activity galaxies in the real groups (field). The fake groups have consistently low averages as compared with the real groups, but this difference is only significant at a 1σ level, as shown by the Gaussian fit to the distribution (solid curve).

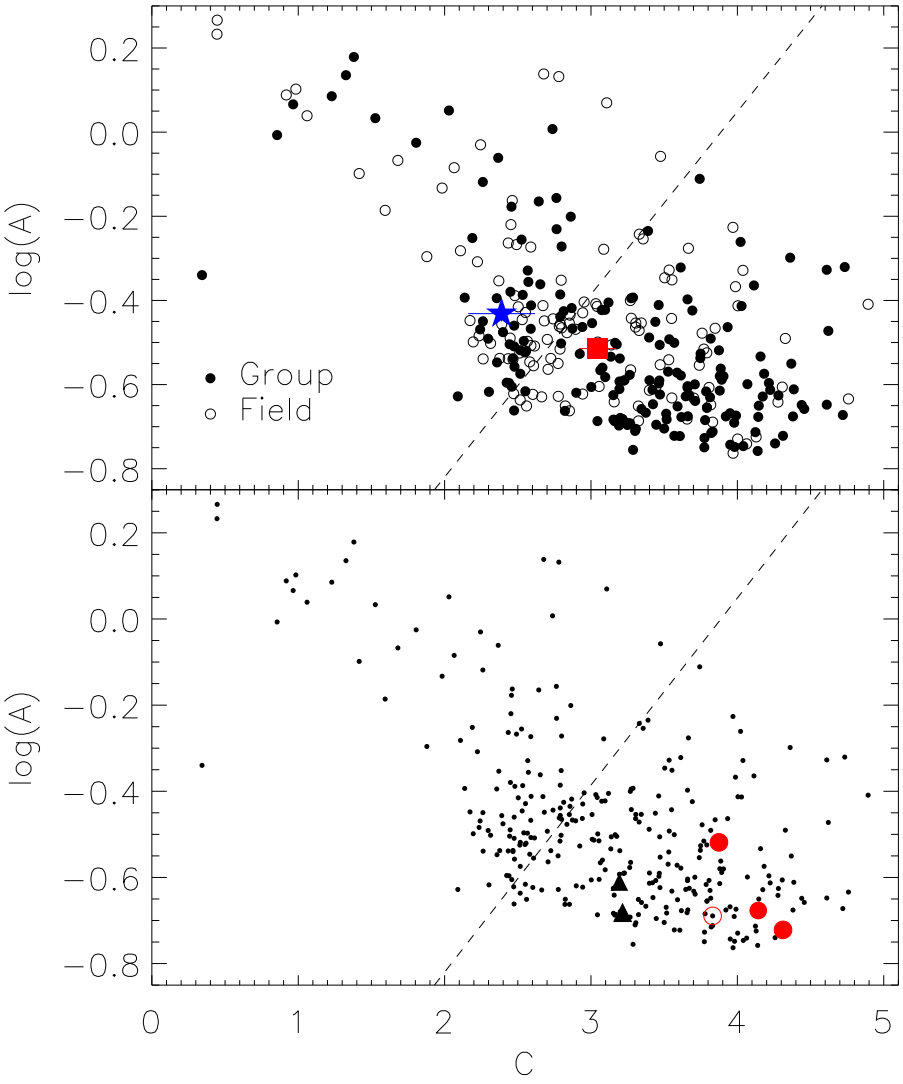

Fig. 9.— Top: asymmetry versus concentration for group (black filled circles) and field (black open circles) galaxies, calculated in the same manner as Shi et al. (2009). These two parameters allow quantitative assessments of galaxy morphology (as opposed to qualitative visual classifications that can be biased by surface brightness dimming). Average values are shown as a red square (groups) and blue star (field), with error bars. The dashed line in both plots is an arbitrary division between the majority of the group and field galaxies, where most of the galaxies below this line are visual early-types and most of the galaxies above this line are late-types. This plot confirms the trend in the visual morphologies: the groups have a higher fraction of early-type galaxies than the field, as shown by the low asymmetry and high concentration of the groups. Bottom: asymmetry versus concentration for group and field galaxies (small black dots), as with the top figure. Our six IR-active E/S0 galaxies are shown as red circles and black triangles, respectively, with group early-types having filled symbols and field galaxies having open symbols. All six E/S0 galaxies fall in the area of the plot populated by early-type galaxies, showing that these IR-active galaxies are indeed early-types.

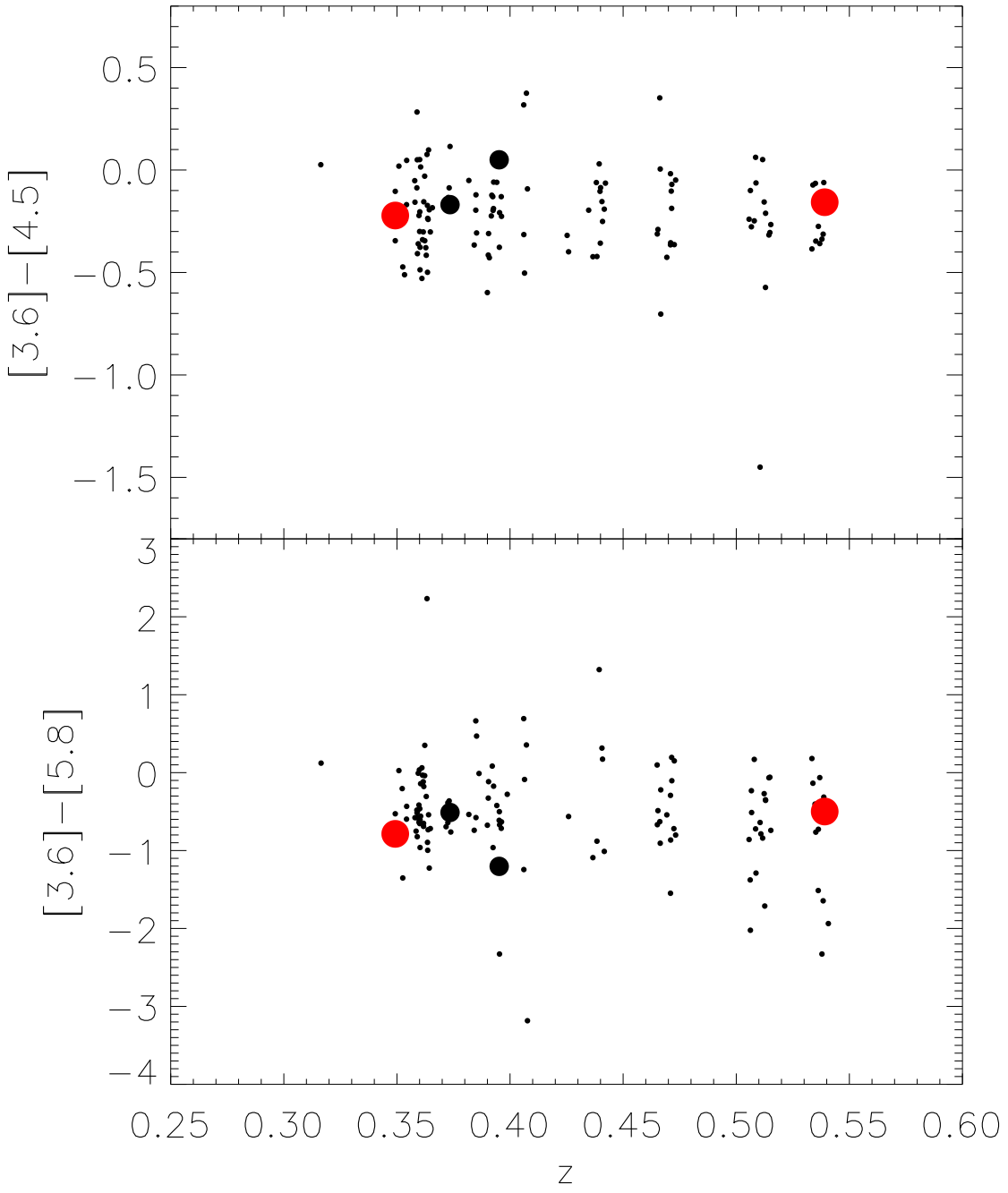

Fig. 10.— IRAC colors [3.6]–[4.5] (top) and [3.6]–[5.8] (bottom) versus z for all galaxies in our sample with IRAC coverage in those bands (small black circles). Also included are four of the six IR-active early-type galaxies that have IRAC coverage. The S0 galaxies are denoted by medium-sized black circles while the ellipticals are denoted by large red circles. Galaxies dominated in these bands by warm dust from an AGN will have highly negative values of [3.6]–[4.5] and [3.6]–[5.8] due to the SED brightening through the IRAC bands. The four E/S0 galaxies with IRAC coverage lie with the rest of the "normal" galaxies, showing that the 24μm emission from these galaxies is dominated by star formation and not AGN activity.

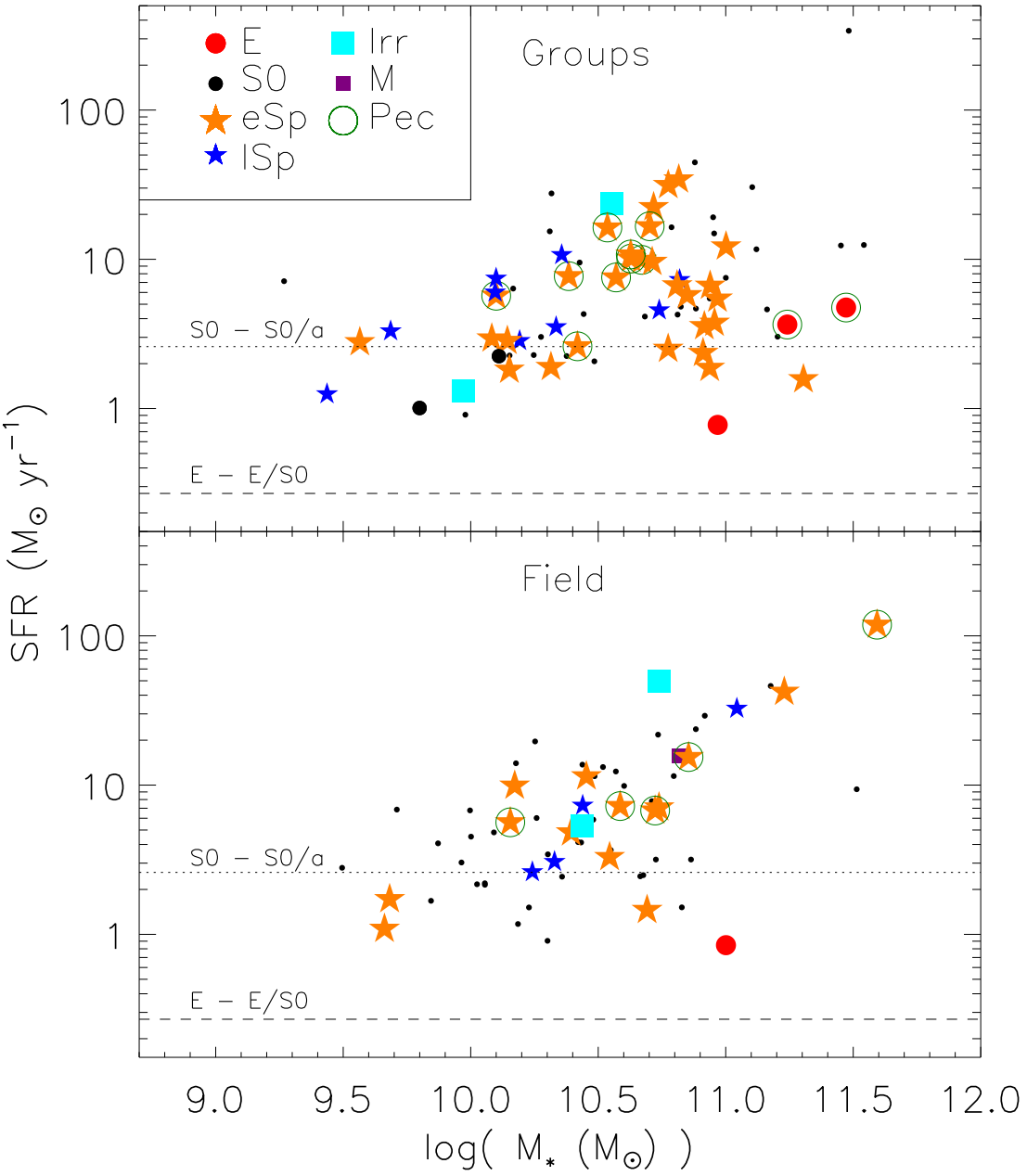

Fig. 11.— SFR versus stellar mass for all galaxies detected at 24μm (small black dots), separated by environment. Visually-classified morphologies, where available, are identified by different point styles and colors. Ellipticals, S0s, and early-type spirals tend to have higher masses than the other galaxy types, as expected. The 99th percentile of 60μm luminosity for E–E/S0 and S0–S0/a galaxies in the Nearby Galaxies Catalog (Tully 1989) correspond to 0.27 $M_\odot$ yr^{-1} (dashed line) and 2.6 $M_\odot$ yr^{-1} (dotted line), respectively. All of the ellipticals detected at 24μm fall far above the SFR seen in local ellipticals, while the two S0s fall close to the 99th percentile for local S0s.

Appendix

Our initial coordinate matching of MIPS 24μm sources to their optical counterparts resulted in 11 early-type (E or S0) galaxies with possible IR emission: seven group and four field galaxies (Table 1). Given the density of galaxies in our fields—and how surprising it was to find E/S0 galaxies with possible star formation—we checked each match individually to confirm whether or not the 24μm emission was coming from the early-type galaxy or if there were a possibility that a close companion was the actual source of the emission. Here, we provide a short description of both the optical and 24μm sources, as well as HST ACS postage stamps of each galaxy (Figure 12) with error circles matched to the 24μm emission at 3 arcsec (matching radius) and 6 arcsec (radius of MIPS PSF FWHM).

PATCH 1447 ID 40969 (Figure 12a): While classified as an "E pec" galaxy (elliptical with a possible interaction from a companion), there are no sources within the 3 arcsec matching radius, and the 24μm emission is clearly right on top of the elliptical (the emission peaks less than 1 arcsec from the center of the elliptical). The 24μm emission is definitely coming from the early-type galaxy with no other obvious source.

PATCH 1447 ID 020364 (Figure 12b): This elliptical galaxy has three small neighbors, though only two are within the 3 arcsec matching radius (the others are slightly farther out). The 24μm source is closer to the nearest neighbor and close to the edge of the 3 arcsec radius. It is possible that the IR emission is coming from the companion galaxy and not the early-type, and so it is not included in our list of IR-active E/S0 galaxies.

PATCH 1447 ID 041307 (Figure 12c): This galaxy is another peculiar elliptical but with no galaxies within 3 arcsec. The 24μm source, while faint, is almost directly on top of the elliptical ($\sim$1 arcsec away). It is highly unlikely that the IR emission is coming from another source, so we classify this galaxy as an IR-active early-type.

PATCH 1447 ID 111706 (Figure 12d): Classified as a normal elliptical galaxy, this source has faint 24μm emission that lies almost on top of the galaxy ($\sim$1 arcsec) with no other obvious galaxies within the match radius. This object has deep X-ray coverage as well, with no detected X-ray source to account for the IR emission. We include this elliptical in our list of star-forming early-type galaxies.

PATCH 1447 ID 122388 (Figure 12e): Other than being classified as an "E/S0," (somewhere between an elliptical and an S0 galaxy, but more closely resembling an elliptical) this galaxy's situation is almost identical to the previous one.

PATCH 1447 ID 150408 (Figure 12f): Here is another regular elliptical galaxy with only one point-source-like neighbor within 3 arcsec. The 24μm source is well within the match

radius, but it is between the nearby object and the elliptical (∼2 arcsec from the elliptical). It is uncertain as to which source the 24μm emission is coming from, so we removed this galaxy from being a star-forming early-type.

PATCH 1447 ID 111547 (Figure 12g): This is a normal elliptical galaxy with two close companions, one of which appears to be a faint irregular fully within the matching radius. The MIPS source appears extended and spans the distance between this closer neighbor and the elliptical. As with the previous galaxy, the uncertainty in the source of the 24μm emission forced us to not include this galaxy as an IR-active source.

PATCH 1447 ID 120982 (Figure 12h): A very faint irregular galaxy barely lies within 3 arcsec of the early-type galaxy, listed as a peculiar S0. The IR source is again between the two galaxies, and though it is slightly closer to the faint companion, the 24μm emission is well within the match radius boundary (∼2 arcsec from the S0). We conservatively do not include this early-type as IR-active.

PATCH 1447 ID 091003 (Figure 12i): This galaxy is an S0/a, meaning it closely resembles an S0 galaxy but with some Sa qualities. There are no other galaxies within 3 arcsec, and the IR source peaks ∼1 arcsec from the S0/a. We include this object as a star-forming early-type galaxy.

PATCH 1447 ID 091304 (Figure 12j): This normal S0 is almost identical to the previous galaxy.

PATCH 1447 ID 141211 (Figure 12k): As with the previous two galaxies, this S0/E (S0 galaxy somewhat similar to an elliptical) has no other companions within 3 arcsec (though there are two faint galaxies between 3.5 and 5 arcsec away). The 24μm emission is slightly offset from the galaxy (∼1 arcsec) but within the match radius. A very faint galaxy lies ∼1.5 arcsec from the 24μm position. While it seems likely that the IR emission is coming from the S0 galaxy, we took a conservative stance and do not classify this galaxy as IR-active.

In Figure 13, we plot rest-frame optical and IR SEDS for the six E/S0 galaxies that have confirmed IR emission. The stellar outputs of these galaxies may be dominated by a relatively old population. Therefore, we fit Rieke et al. (2009) average star-forming galaxy templates to the SEDs in two distinct segments. First, we found the average template with the closest L_{TIR} to each galaxy and fit the 24μm data point to the template (red spectrum). For the normal stellar emission, we used optical and near-IR photometry to find the best-fit (χ^2) average star-forming template (orange spectrum). Except for the first two galaxies, we see a clear stellar bump from normal stars and then increasing luminosity of the mid-IR dust emission beyond 7μm, indicative of a normal star-forming galaxy and not an AGN. In all cases, the SED is consistent with the expectation for star formation. There are two cases

where 1) there is IRAC data; and 2) a detection of the aromatic emission at 8μm is predicted from the combination of IRAC bands 1–3 and the MIPS 24μm flux density. The expected 8μm excess is seen for both galaxies.

Table 1. Early-Type Galaxies Matched with IR Sources

Patch[a]	ID	R.A.	Decl.	z	L_{TIR} (10^{10} $L_\odot$)	SFR ($M_\odot$ yr^{-1})	Group[b]	Galaxy Type	X-ray Coverage?
1447	040969	222.377813	9.511117	0.35	3.8	3.7	23	E pec	N
1447	020364	222.431575	9.232753	0.36	11	12	25	E	N
1447	041307	222.427158	9.536456	0.54	4.9	4.8	39	E pec	N
1447	111706	222.483754	8.940261	0.39	0.89	0.78	32	E	Y
1447	122388	222.355163	9.074511	0.41	0.96	0.85	0	E/S0	Y
1447	150408	222.184342	8.842967	0.32	1.7	1.5	0	E	N
1447	111547	222.470204	8.926272	0.30	1.0	0.91	0	E	Y
1447	120982	222.349458	8.990908	0.37	3.0	2.8	0	S0 pec	Y
1447	091003	222.578538	9.010039	0.40	1.1	1.0	32	S0/a	N
1447	091304	222.578025	9.030156	0.37	2.4	2.2	28	S0	N
2148	141211	327.600550	-5.681283	0.44	4.5	4.3	138	S0/E	Y

[a]Original CNOC2 patch number (Yee et al. 2000).

[b]Galaxy group to which the object belongs; a 0 value indicates a field galaxy.

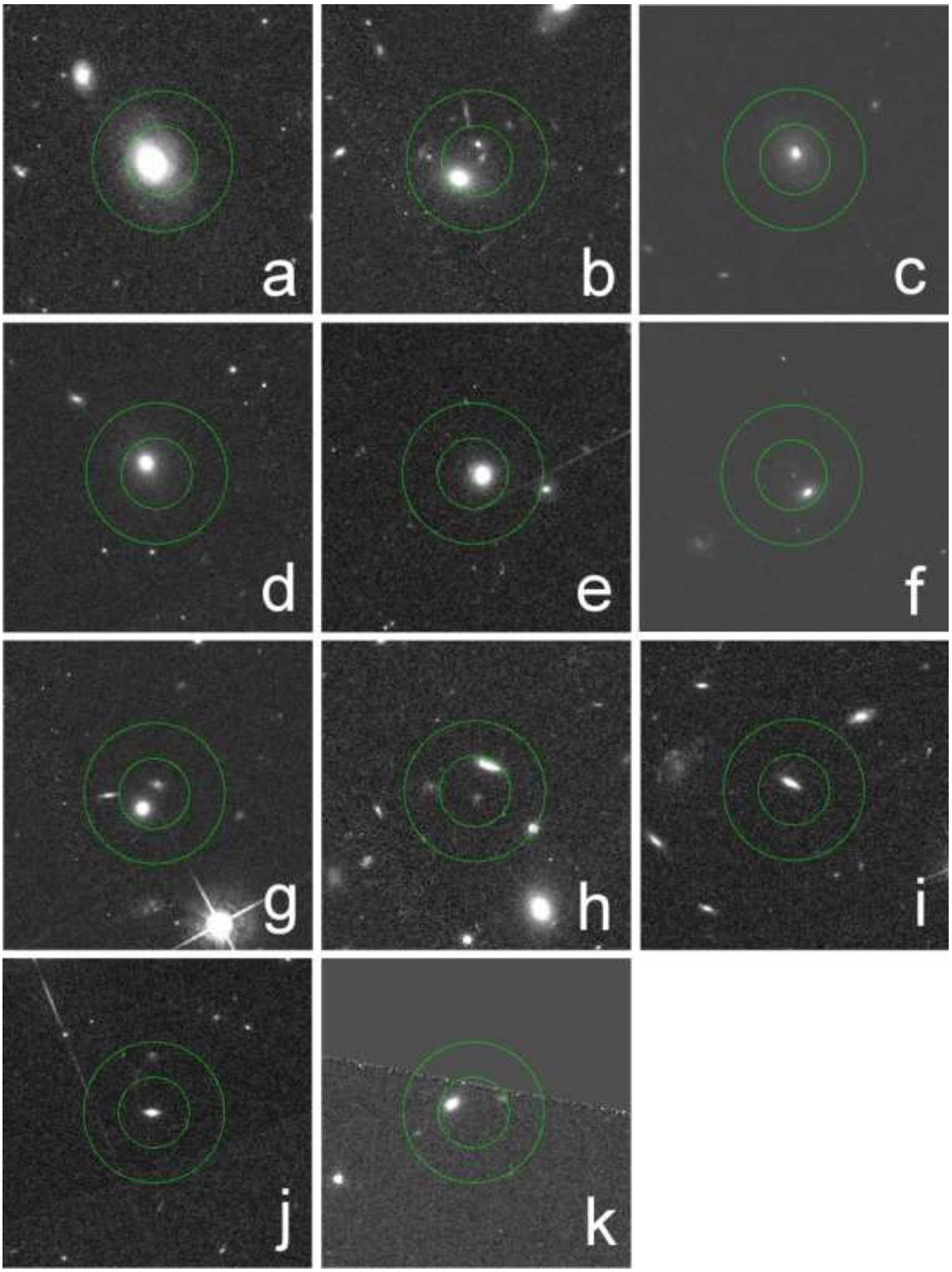

Fig. 12.— HST ACS images of the 11 E/S0 galaxies matched with 24μm sources. The inner annulus has a radius of 3 arcsec, which is the length we used for matching the optical coordinates with 24μm sources. The outer annulus shows the FWHM of the MIPS PSF. The ID and patch number of the matched galaxies are as follows: (a) 1447 040969, (b) 1447 020364, (c) 1447 041307, (d) 1447 111706, (e) 1447 122388, (f) 1447 150408, (g) 1447 111547, (h) 1447 120982, (i) 1447 091003, (j) 1447 091304, and (k) 2148 141211.

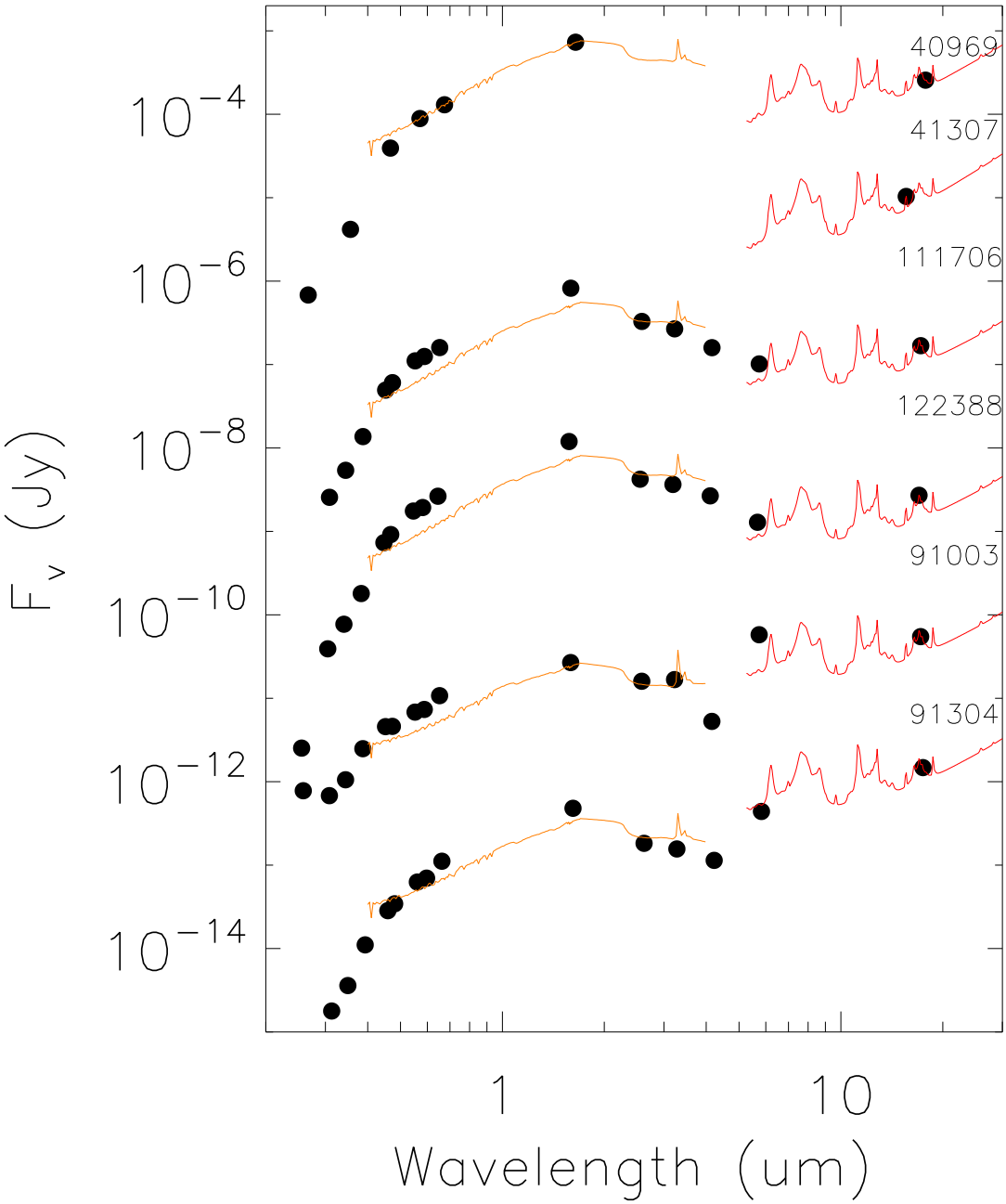

Fig. 13.— Optical and IR SEDs (rest-frame) for all six star-forming E/S0 galaxies, identified by their GEEC ID and fit by different segments of the Rieke et al. (2009) average star-forming galaxy templates. Each galaxy was matched to the average template with the closest L_{TIR} and fit to the 24μm data point (red spectra). The orange spectra are best-fit (χ^2) average star-forming templates for the optical/near-IR photometry; while these fits are not very accurate, they are sufficient for our purposes. Except for 40969 and 41307, all galaxies have enough photometric points to indicate the presence of a stellar bump and mid-IR dust emission similar to normal star-forming galaxies.